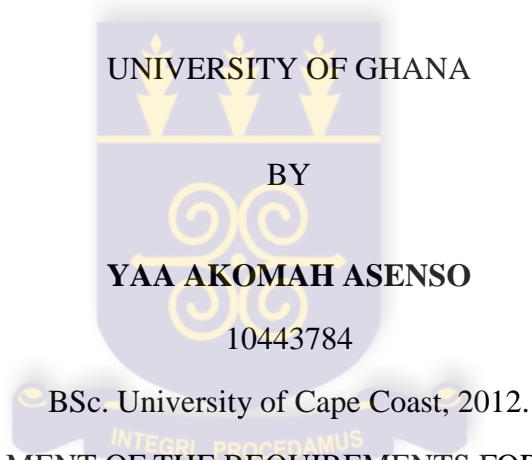


**PERFORMANCE EVALUATION AND DOSE VERIFICATION OF THE LOW
DOSE RATE PERMANENT PROSTATE BRACHYTHERAPY SYSTEM AT THE
KORLE-BU TEACHING HOSPITAL**

A THESIS PRESENTED TO THE
DEPARTMENT OF MEDICAL PHYSICS

SCHOOL OF NUCLEAR AND ALLIED SCIENCES



IN PARTIAL FULFILMENT OF THE REQUIREMENTS FOR THE AWARD OF

MASTER OF PHILOSOPHY DEGREE

IN

MEDICAL PHYSICS

JULY, 2015

DECLARATION

Student's Declaration:

I hereby declare that, with the exception of references to other people's work which have been duly acknowledged, this work is the result of my own research undertaken under supervision, and either in whole or in part has not been presented for any other degree at another university elsewhere.

.....
Yaa Akomah Asenso
(Student)  Date

.....
Prof. Cyril Schandorf
(Principal Supervisor)  Date

.....
Mr. Francis Hasford
(Co-Supervisor) Date

.....
Mr. Samuel Nii Adu Tagoe
(Co-supervisor) Date

ABSTRACT

Low dose rate prostate brachytherapy equipment that is newly acquired or substantially upgraded requires acceptance testing before being put into clinical service as well as Quality control after installation and when in use. Thus, quality control tests typically are periodic repetitions, partial or full, of acceptance and commissioning tests. The ultrasound system is the most important equipment used in LDR prostate brachytherapy. The AAPM TG 128 provide a set of instructions for quality control testing of an ultrasound system with a specific focus on those tests applicable to image guidance during a prostate implant procedure. Following the AAPM TG 128 protocol and CIRS 045 brachytherapy QA phantom as well as other protocols, eight experiments were performed to evaluate the performance of the system. The overall average axial distance in the B and F columns were found to be 10.12 ± 0.1 mm and 10.10 ± 0.11 mm respectively deviating by approximately 1.2 % and 1.0 % respectively from a standard inter- target distance of 10 mm. Also the lateral distance measured along the rows 1, 2, 3 and 4 resulted in an average distance of 10.07 ± 0.06 mm along rows B4 – C4, deviating from the standard inter- target distance of 10 mm by approximately 0.07 mm or ± 0.7 %, that of B3 – D3 also was 20.01 ± 0.07 , deviating from 20 mm standard inter- target distance by 0.01 mm or 0.05 %, targets along B2 – E2 recorded an average distance of 29.56 ± 0.33 mm deviating from 30 mm standard inter- target distance by approximately -0.44 mm or -1.47 % and the last which is B1 – F1 also recorded an average distance of 39.54 ± 0.38 mm deviating from 40 mm standard inter- target distance by approximately -0.46 mm or - 1.15 %.

Volume measurement accuracy of the three standard volumes, 4 cm³, 9 cm³ and 20 cm³ produced average measurements of 3.97 ± 0.16 cm³, 8.86 ± 0.29 cm³ and 20.11 ± 1.04 cm³ resulting in approximate deviations of -0.75 %, -1.56 % and 0.55 % respectively. That of the physical and internal grid alignment yielded a maximum discrepancy of 2.67 ± 0.01 mm at position 6A on the template. The probe retraction test produced no discrepancies in the “clicks” and corresponding distances. Meanwhile the depth of penetration and axial and lateral resolution test at the time performing the tests were no available standard measurements for comparison. The dose verification test consisted of three tests, the calibration point test, the source strength verification and the TPS dose verification. The calibration point test indicated that distance for maximum ionization chamber sensitivity is 3cm, so seeds can be calibrated at this point. The source strength verification were within the tolerances recommended by ICRU report 38 (ICRU, 1985). The average source strength measured was 0.651450 U \pm 0.001052 U deviating from the manufacturer value of 0.64989 U by 0.242 % \pm 0.164 %. The TPS dose verification test produced results with significant errors which occurred due to post irradiation development of film with time but the doses obtained by both TPS and film followed the same pattern. The outcome of the performance evaluations indicate that for patient work, the ultrasound system and prostate brachytherapy system can provide the mechanism for accurate positioning of the brachytherapy seeds facilitating reliable identification of the target volume for accurate effective treatment.

DEDICATION

I first and foremost dedicate this work to God Almighty. Secondly, to my dear parents; Mr. and Mrs. Asenso Mensah and thirdly to my sister Akua Asaa for all their support, love and care.



ACKNOWLEDGEMENT

To God is the glory for His strength, wisdom, protection, guidance and divine favour given me throughout this research study to reach a successful end.

The success of this research work would not have been successful without the efforts of my committed supervisors Professor Cyril Schandorf, (Department of Medical Physics), Professor A.W.K. Kyere (Head of department, Medical physics), Mr. Francis Hasford (Department of Medical Physics) and Mr. Nii Adu Tagoe (School of Allied and Health science, University of Ghana) for their tremendous advice, guidance and great encouragement throughout this study.

I would also like to appreciate the staff of medical physics department at Korle-Bu Teaching Hospital for their support and allowing to me to use the equipment and materials in the Department.

I would like to acknowledge two of my course mates, Mr. Philip Odonkor and Mr. Ainadine Ebraimo Momade for their support and help in finishing this thesis.

I will also commend the works of all lecturers who have contributed to making the MPhil. Medical Physics program a success.

God richly bless you all.

TABLE OF CONTENTS

DECLARATION	ii
ABSTRACT	iii
ACKNOWLEDGEMENT	vi
ABBREVIATIONS	xii
CHAPTER ONE	1
INTRODUCTION	1
1.1 Background	1
1.2 Statement of problem	5
1.3 Objective of the study	6
1.4 Relevance and justification	7
1.5 Scope and delimitation	7
1.6 Organization of thesis	8
CHAPTER TWO	9
LITERATURE REVIEW	9
2.1 History of permanent prostate implants	9
2.2 Dose rate prostate brachytherapy systems	10
2.2.1 The LDR brachytherapy systems	10
2.2.1.1 Radioisotopes used in LDR prostate brachytherapy	10
2.2.1.1.1 Iodine- 125 seed source	11
2.2.1.1.2 Palladium-103 seed source	13
2.2.1.2 Transrectal ultrasound prostate brachytherapy	16
2.2.1.2.1 Transrectal ultrasound system (TRUS)	17
2.2.2 The HDR brachytherapy system	18
2.2.2.1 Radionuclides used in HDR brachytherapy systems	18
2.2.2.1.1 Iridium -192	18
2.2.2.2 Afterloading system	19
2.3 Acceptance testing, commissioning and quality control of LDR prostate brachytherapy systems	20
2.3.1 Acceptance testing of LDR prostate brachytherapy system	21
2.3.2 Commissioning of LDR prostate brachytherapy system	23

2.3.3 Quality control of LDR prostate brachytherapy system.	24
2.4 Treatment planning and dosimetry of LDR prostate brachytherapy systems.	24
2.4.1 Interstitial implants	24
2.4.2 Postimplant dosimetry	25
2.4.3 Computerised dosimetry.	26
2.4.4 Treatment planning system.	28
2.4.5 AAPM TG-43 formalism	29
2.4.5.1 Application of TG-43 to I-125 dosimetry	32
2.5 Performance evaluation protocols for LDR prostate brachytherapy systems.	34
CHAPTER THREE	36
MATERIALS AND METHOD.....	36
3.1 Performance evaluation of the transrectal ultrasound system.....	36
3.1.1 Materials and equipment.....	36
3.1.1.1 Brachytherapy QA phantom (CIRS model 045).....	36
3.1.1.2 Transrectal ultrasound system (B-K Medical-Falcon 2101 EXL)	38
3.1.1.3 Gel.....	42
3.1.1.4 Implant needles	42
3.1.2 Performance evaluation tests	43
A. “N” Target group	44
A.1 lateral and axial distance measurements	45
A.2 Internal grid / template grid alignment.....	46
A.3 Lateral and axial resolution test	47
B. Volume targets	48
C. Cross axis group.....	49
3.2 Dose verification tests.....	49
3.2.1 Materials and equipment.....	50
3.2.1.1 I- 125 seed source	50
3.2.1.2 Gafchromic EBT2 1417 film	52
3.2.1.3 Perspex prostate phantom	52
3.2.1.4 Prowess panther (v 4.5).....	54
3.2.1.5 ImageJ software	54
3.2.1.6 Ionization chamber (HDR 1000 Plus well chamber) and electrometer (MAX 4000)55	

3.2.2 Dose verification tests	56
3.2.2.1 Determination of calibration point of the well chamber.	56
3.2.2.2 Verification of source strength.....	57
3.2.2.3 Treatment planning dose verification.....	59
CHAPTER FOUR.....	61
RESULTS AND DISCUSSION	61
4.1 Performance evaluation results	61
4.1.1 Axial distance measurement accuracy	61
4.1.2 Lateral distance measurement accuracy.....	63
4.1.3 Volume measurement accuracy	65
4.1.4 Depth of penetration (DOP).....	66
4.1.5 Axial and lateral resolution accuracy	67
4.1.6 Physical grid alignment accuracy/ internal grid alignment accuracy.....	68
4.1.7 Probe retraction accuracy.....	70
4.2 TPS dose verification results	70
4.2.1 Calibration point test.....	71
4.2.2 Source strength verification test.....	72
4.2.3 Treatment planning dose verification test	73
4.3 Limitation.....	77
CHAPTER FIVE	79
CONCLUSION AND RECOMMENDATION.....	79
5.1 Conclusion	79
5.2 Recommendation	80
5.2.1 National Centre for Radiotherapy and Nuclear Medicine.....	81
5.2.2 Regulatory Authority	81
REFERENCES	83
APPENDIX.....	90

LIST OF PLATES

Plate 3.1: The CIRS model 045 brachytherapy QA phantom.....	37
Plate 3.2: The B – K transrectal ultrasound system	39
Plate 3.3: The rectal probe used in this work.....	40
Plate 3.4: The template grid	40
Plate 3.5: The stepper with the probe and template holders	41
Plate 3.6: The stepper, probe and template mounted on the stabilizing mechanism	41
Plate 3.7: The implant needles used in this work.....	43
Plate 3.8: The set up for performance evaluation measurements	44
Plate 3.9: The ultrasound image showing the “N” target group	45
Plate 3.10: The set up for the template grid alignment test	47
Plate 3.11a: Pictures of the loose seeds	51
Plate 3.11b: The seed cartridge.....	51
Plate 3.11c: The screw- cap vial	51
Plate 3.12: The perspex prostate phantom	53
Plate 3.13: The user interface of the prowess panther	54
Plate 3.14: An opened view of ImageJ user interface.....	55
Plate 3.15: The electrometer and well chamber used	56
Plate 3.16: The source holder.....	57
Plate 4.1a: Axial measurement on column B.....	62
Plate 4.1b: Axial measurement on column F.....	62
Plate 4.2: Lateral distance measurement along B1 – F1	64
Plate 4.3: Measurement of volume targets.....	66
Plate 4.4a: Ultrasound image of the needles	69
Plate 4.4b: Set up for grid alignment accuracy.....	69
Plate 4.5: A CT slice of the Perspex prostate phantom showing the calculation points...	76

LIST OF FIGURES

Figure 2.1: I – 125 decay diagram	13
Figure 2.2: Pd – 103 decay diagram	15
Figure 2.3: Ir – 192 decay scheme	19
Figure 2.4: Geometry and coordinate definations used in the TG – 43 dosimetry protocol.	30
Figure 3.1: The schematic diagram of the QA phantom.....	38
Figure 4.1: A graph of current (mA) against position (cm).....	72
Figure 4.2: The dose response curve for the calibrated Gafchromic EBT2 film.....	74
Figure 4.3: A graph showing the difference in TPS and measured dose.....	76

ABBREVIATIONS

2-D	Two dimensional
^{103}Pd	Palladium - 103
^{102}Pd	Palladium - 102
^{125}I	Iodine - 125
^{124}X	Xenon - 124
^{131}Cs	Cesium - 131
AAPM	American association of physics in medicine
ABS	American brachytherapy society
ADCL	Accredited dosimetry calibration laboratory
AIUM	American institute of ultrasound in medicine
Bq	Becquerel
CaP	Prostate cancer
CAPCA	Canadian association of provincial cancer agencies
Ci	Curie
CRP	Co-ordinated research project
CT	Computed tomography
DRE	Digital rectal examination
DVH	Dose volume histogram
EBRT	External beam radiation therapy
ESTRO	European society of therapeutic radiology and oncology
eV	Electron volts
g	gram
GBq	Gigabequerel
Gy	Gray
HDR	High dose rate

IAEA	International atomic energy agency
ICRU	International commission of radiological units
ISO	International standards organization
KeV	Kiloelectron volts
KBTH	Korle – Bu Teaching Hospital
LDR	Low dose rate
MBq	Megabequerel
mCi	Millicurie
MPD	Matched peripheral dose
NCRP	National commission on radiation protection
NIST	National institute of standards and Technology
PSA	Prostatic specific antigen
PVC	Polyvinyl chloride
QA	Quality assurance
QC	Quality control
RPC	Radiological physics center
TG	Task group
Ti	Titanium
TPS	Treatment planning system
TRUS	Transrectal ultrasound system
USA	United States of America
U	$\mu\text{Gym}^2/\text{h}$
MSKCC	Memorial Sloan Kettering Cancer Center
NCS	Nederlandse Commissie voor Stralings dosimetrie
AES	America Endocurietherapy Society

CHAPTER ONE

INTRODUCTION

1.1 Background

The prostate is a gland that is a part of the male reproductive system that wraps around the male urethra near the bladder. Prostate cancer (CaP) has the highest prevalence of any non-skin cancer in the human body. Essentially all men with circulating androgens will develop microscopic CaP if they live long enough. The factors that determine the risk of developing clinical CaP are not well known, although a few have been identified. There are three well established risk factors for CaP which include, increasing age, hereditary and ethnicity (Heidenreich et al, 2012). According to age, 60% of cases of CaP arise in men over 65 years of age (Davis, 2014). The disease is rare in men under 40 years. Therefore, the older a man is, the greater his risk of getting CaP.

The diagnosis of prostate cancer most commonly involves a combination of three tests, the digital rectal examination (DRE), prostatic specific antigen (PSA) blood test and prostate biopsy.

Brachytherapy has gained wide acceptance as a treatment modality for early stage prostate cancer, in which the disease is confined to the prostate gland. Brachytherapy is a radiation therapy treatment modality commonly used for the treatment of cancer. The term 'brachy' implies short distance treatment as opposed to external beam radiation therapy (EBRT), or teletherapy, where treatment is delivered from a distance. Brachytherapy makes use of discrete, encapsulated gamma sources that can be placed into or immediately adjacent to the tissue to be treated, allowing the delivery of a high

localized radiation dose in the tumour. The intensity of the source decreases according to the inverse square law resulting in a rapid dose fall off at short distances from the sources. The significance of the rapid dose fall off in brachytherapy is that a highly localized dose can be delivered directly to the tumour, while the surrounding normal tissue receives only a small fraction of the total dose. For this reason, brachytherapy allows higher doses per fraction to be delivered to the tumour, compared to the standard 2 gray (Gy) per fraction used in EBRT (Wilkinson, 2010). In brachytherapy, most radionuclides used are photon emitters however; beta or even neutron emitting sources are used for source applications.

The practice of brachytherapy first began following the discovery of radium by Marie Curie in 1898, where patients were treated using small quantities of radium placed on or implanted into tumours (Wilkinson, 2010; Godden, 1988). Brachytherapy has evolved over the years with the introduction of a variety of new radionuclides for brachytherapy, the use of remote after loading units and computer based dose calculation systems.

The two main brachytherapy implant techniques used in modern day treatment are:

- Intracavitary: Sources are arranged in a suitable applicator to irradiate the walls of a body cavity from inside, in effect the sources are placed in the heart of the tumour. This method is mostly used for cancers of the uterine, cervix, uterine body and vagina. Inserts are always temporal.
- Interstitial: Radioactive sources are fabricated in the form of needles, wires, or seeds that are implanted directly into the diseased tissues. Inserts can either be permanent or temporal.

Other less common forms of brachytherapy treatments include surface plaque, intraluminal, intraoperative and intravascular source applications; for these treatments either gamma or beta emitting sources are used.

Several aspects must be considered when giving brachytherapy treatments. Of importance is the way in which the sources are positioned relative to the volume to be treated, and several different models have been developed over the past decades for this purpose. The advantages of using a well-established model is that one benefits from the long experience associated with such models and that one can take advantage of published results. The use of uniform models and methods in brachytherapy treatments simplifies comparison of treatment results (Suntharalingam et al, 2005). For the purpose of this study, a constant source strength but different source positioning will be employed. Therefore the Paris model/system will be of much benefit. However, the use of a model alone is not sufficient to validate results. It is necessary to have a reliable method for determination of the source strength in order for the dose calculation to be accurate. This means that it is necessary for brachytherapy sources to be calibrated, with the calibration traceable to a national or international standards laboratory.

Prostate brachytherapy can be delivered with differing dose rates. Low dose rate (LDR) prostate brachytherapy involves the insertion of radioactive seeds under ultrasound guidance into the prostate to achieve a conformal high dose of radiation to the prostate. It is usually given as a monotherapy but can be used as a boost to external beam radiotherapy (EBRT). With LDR prostate brachytherapy as described by the board of the faculty of clinical oncology, the Royal College of Radiologist, the seeds are left in situ

permanently and emit radiation gradually over several months (The Royal College of Radiologist).

In contrast, high dose rate (HDR) prostate brachytherapy is predominantly used as a boost to EBRT. Catheters are positioned within the prostate using ultrasound guidance and the planned treatment is delivered using a remote after loading unit with a single iridium-192 stepping source. The number of fractions in current schedules varies between one and four.

The focus of this study is LDR prostate brachytherapy based on permanent interstitial implants. This system is typically a radioisotope delivery unit with an ultrasound probe driven mechanism (stepper), applicators, an ultrasound machine, template grid and a VariSeed[®] brachytherapy treatment planning system. Low dose rate (LDR) brachytherapy uses an implanted source that delivers a dose of 40 to 60 cGy per hour over several days. After the treatment parameters have been tested, the stepper advances the source from its stand, which is guided by an ultrasound system to ensure accurate source placement.

Early diagnosis, primarily due to more widespread PSA screening, has resulted in more patients being diagnosed with early stage disease (Lawton et al, 1998; Stamey et al, 1987). For a disease that is likely confined to the prostate and the immediate surrounding area, surgery, external beam radiation (EBRT) and seed implantation are the primary treatment options. In recent years, seed implantation has become more popular as a treatment option. It has been estimated that up to 50% of patients with early stage prostate cancer are now receiving ultrasound-guided seed implantation. This rise in

popularity is most likely due to (i) the fact that five- and ten-year disease control rates of brachytherapy equal those of the top surgical and radiation series, (ii) the toxicity and side-effects are perceived to be lower, and (iii) the brachytherapy involves just a single outpatient treatment. Implants are used for early stage cancers (Khan, 2003). However, patients with extensive tumors (TNM stage T3 and T4) are not good candidates for implantation.

1.2 Statement of problem

The aim of radiotherapy is to give maximal dose to the tumor whilst reducing dose as much as possible to the normal surrounding tissues. A treatment does not reach its goals if the source misses its aimed positions by a large margin; that is, if there are severe geographical misses in placing the sources relative to their intended positions. Owing to the steep dose gradient that characterizes brachytherapy such geometrical misses may be seriously detrimental to patient and would affect treatment outcome. Thus there is a need for a quality control program guaranteeing that the treatment is given in accordance with its purpose. Image guided prostate brachytherapy has grown in importance as a valuable tool in the treatment of prostate cancer. Often overlooked in a brachytherapy program is the ultrasound system itself, frequently receiving no more attention than, perhaps, a superficial preventive maintenance by a service or biomedical engineer. Korle Bu Teaching Hospital in Accra, Ghana faces the same operational problems. Since the acquisition of the brachytherapy system including the imaging system (ultrasound machine), the stepper, and the template grid at the hospital there has not been any acceptance testing or commissioning tests of the system to receive it into clinical use.

This was due to the unavailability of a QA phantom at the hospital at the time of purchase of ultrasound system and the prostate brachytherapy system.

This research is therefore being conducted to evaluate the performance of the prostate brachytherapy system and its associated treatment planning.

.

1.3 Objective of the study

The main goal of this work is to evaluate the performance of ultrasound system and the permanent prostate brachytherapy system to verify whether it meets the standards to be used in the clinical setting for prostate cancer treatment. The specific objectives are:

1. To establish procedures for accurate visualization of the prostate and other critical structures with the ability to identify the locations of the inserted seeds using the quality assurance phantom acquired.
2. To establish procedures to ensure that the grid patterns of the ultrasound image correspond to the physical locations given by the template.
3. To establish procedures to ensure that the treatment planning system reproduces the dose at total decay from an I-125 source.
4. To establish procedures to ensure accurate volume measurements for preoperative dosimetric planning.
5. To assess and reduce dosimetric uncertainties to acceptable levels.
6. To develop a QC program in the area of permanent prostate brachytherapy for routine clinical use at the Korle Bu Teaching Hospital.
7. To make appropriate recommendation to relevant stakeholders.

1.4 Relevance and justification

The outcome of this research work can be used to verify the actual position of seeds and compared to the pre-plan by the oncologists if there are any discrepancies to ensure the accurate positioning of seeds hence ensuring better treatment outcome and quality of life. It will also help in accurately positioning each needle in a three dimensional co-ordinate system exactly at a place determined in advance by preplanning procedure. The findings of this research work will serve as guide and protocol for oncologists, radiographers, medical physicist, dosimetrist and other related medical professionals at the Korle- Bu Teaching Hospital.

The International Atomic Energy Agency (IAEA) has projects among its member States including Ghana that seeks to strengthen radiological protection of patients; hence findings from this study will be of relevance nationally and internationally.

1.5 Scope and delimitation

This work was carried out at Korle-Bu Teaching Hospital in Accra, Ghana. It was limited to LDR prostate brachytherapy system at the radiotherapy department of the hospital. The research and protocol development included vertical and horizontal resolution, vertical and horizontal distance accuracy, internal grid/template assessment, probe retraction step assessment, depth of penetration, volume verification and calculated dose verification.

1.6 Organization of thesis

This research work write up covers five chapters. Chapter one focuses on the introduction to the study. Chapter two reviews existing literature relating to the research problem. Chapter three focuses on the materials and methodology of the study. Chapter four contains the results and discussions, while chapter five provides the conclusions and recommendations from the overall findings. The references section contains all the relevant works cited throughout the thesis.

CHAPTER TWO

LITERATURE REVIEW

This chapter focuses on the review of existing literature relevant to this research work.

2.1 History of permanent prostate implants

Seed implantation for prostate cancer was originally suggested by Alexander Graham Bell as far back as 1903 (Grimm et al, 2003). In 1911, Louis Pasteur suggested that the insertion of radium into the prostate may eradicate this malignancy (Pasteau, 1911). Various techniques were subsequently employed with limited success. In the 1960s, Drs. Scardino and Carlton reintroduced permanent prostate brachytherapy using 198-Au (gold-198) interstitial implantation combined with external beam radiation therapy. At about the same time, Dr. Whitmore and colleagues at Memorial Sloan Kettering Cancer Center (MSKCC) also began to insert I-125 seeds through an open incision as a sole treatment. Unfortunately, these early techniques did not allow for clear visualization of the seeds as they were being inserted into the prostate and, as a result, there was often poor dose coverage of the gland (Lawton et al, 1998; Fuks et al, 1991).

Despite the limitations of these techniques, some important information was obtained from the early seed implant approaches. Local cancer control was better in patients who received high quality implants and who had low grade and early stage cancer. The group from MSKCC reported a 60% local control rate in those patients who received prescription doses of > 140 Gy (Gray) versus 20 % if the dose was less than 140Gy. The 15-year survival was 70% in patients with stage B1 prostate cancer treated with I-125

seed brachytherapy (Grimm et al, 2003). These results suggested strongly that seed placement and proper patient selection were important determinants of cancer control. The subsequent development of the transperineal, ultrasound guided approach provided a means for more accurate placement of seeds and thereby improve dose coverage.

2.2 Dose rate prostate brachytherapy systems.

There are two types of brachytherapy that are used in the treatment of prostate cancer: permanent low dose radiation (LDR) and temporary high dose radiation (HDR).

2.2.1 The LDR brachytherapy systems

LDR brachytherapy uses iodine-125 and palladium -103 stored in titanium case usually referred to as brachytherapy seeds. As the name permanent brachytherapy suggests, the seeds are permanently left inside the prostate gland. Over the course of their radioactive lives, the seed will continuously emit low radiations until they decay completely. The LDR brachytherapy systems include the radioisotopes and system for implantation.

2.2.1.1 Radioisotopes used in LDR prostate brachytherapy.

The modern brachytherapy seed was introduced in 1965 (Aronowitz et al, 2013). Multiple manufacturers have since produced ^{125}I as well as ^{103}Pd and ^{131}Cs seeds. While surface variations (such as damping, to enhance echogenicity) have been employed, the seed dimensions have essentially been maintained. However, a thinner (0.5mm diameter)

^{125}I seed that can pass through a 20-gauge needle has been introduced and is being evaluated to determine if the smaller puncture would deduce urinary and sexual toxicity (Aronowitz et al, 2013). ^{125}I and ^{103}Pd are the most common radioactive isotopes used for prostate seed implant. Based on their decay rates, ^{125}I and ^{103}Pd have been prescribed to tumors considered slow-growing and fast-growing as designated by their Gleason grade respectively (Ling et al., 1995). At the Korle Bu Teaching Hospital, the radionuclide used for prostate brachytherapy treatment is the Iodine-125.

2.1.1.1.1 Iodine- 125 seed source

^{125}I is routinely produced by thermal neutron irradiation of ^{124}Xe gas; activity concentration is as high as 3.7GBqmm^{-3} can be obtained by encapsulating an iodide-activated ion exchange bead (Mayles et al., 2007). ^{125}I decays via electron capture (Khan, 2003, IAEA 2006). This isotope is mainly supplied by enriched isotope producing companies on a regular commercial basis. The ^{125}I source core usually consists of silver backing which acts as an x-ray marker, with the radionuclide activity fixed on its surface. In some cases ceramic support is used. Titanium is a unique material, as strong as steel but its weight, with excellent corrosion resistance. The high strength, low weight and outstanding corrosion resistance possessed by titanium has led to its choice as the capsule material.

^{125}I sources are used in brachytherapy of brain, neck, lung, pancreas and prostate cancers, as well as intraocular tumours (choroidal melanomas and retinoblastoma). They can be used in two different ways – permanent and temporary implants. ^{125}I seeds are indicated

for the treatment of tumours that have the following characteristics: localized, slow growth rate and low to moderate ratio sensitivity. They are also indicated for the treatment of recurrent tumours and residual tumours following a course of external radiation therapy. Required activity of ^{125}I seed used in ophthalmic application is, on average, 20mCi (740MBq) and in other applications most often 4- 5mCi (148-185MBq). It is highly encouraging to know that brachytherapy using ^{125}I sources has been effective in the treatment of prostate cancer.

The ^{125}I I decay scheme (figure 2.1) results in the emission of photons with energies of 27.4 keV (1.15 photons/disintegration), 31.4 keV (0.25/dis) and 35.5 keV (0.067/dis) (Yu et al, 1999). The average energy for all emissions is approximately 27.4 keV, which results in a half value layer in lead of approximately 0.025 mm (Yu et al, 1999). The half life of ^{125}I is 59.4 days; ninety percent of the total dose is delivered in 197 days. When implanted in the patients, it takes approximately 204 days for 90% of the prescribed dose to decay (Rivard et al., 2007).

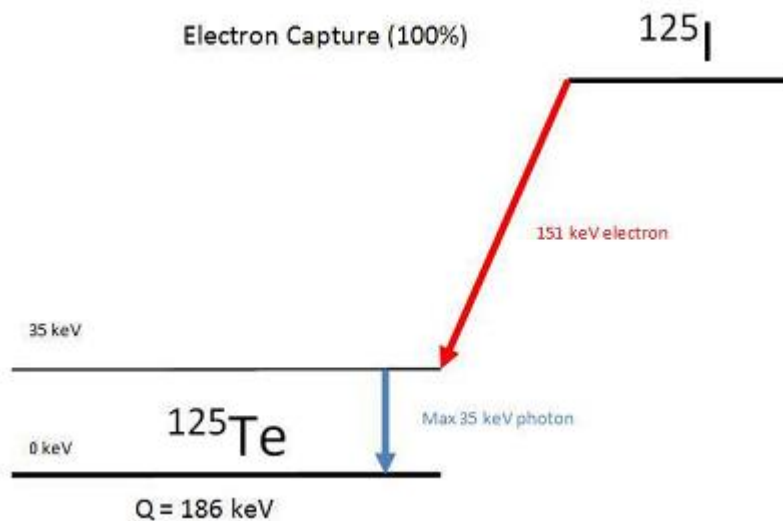


Figure 2.1: I-125 decay diagram

2.2.1.1.2 Palladium-103 seed source.

^{103}Pd is commonly produced by cyclotron irradiation of rhodium targets with accelerated protons. This approach allows production of carrier-free palladium-103 having near theoretical value of specific activity of 75000 Ci/g ($\sim 2.8 \times 10^6$ GBq/g). Nevertheless, carrier (metal palladium) is commonly added to stabilize its behavior at isolation/purification from radioactive impurities and at seed core production, as well. In such a case the ^{103}Pd specific activity decreases, but it should be at least 5 Ci/g (185 GBq/g) for successful source production. The disadvantage of cyclotron production of ^{103}Pd is the relatively high price of this radioisotope.

An alternative approach to ^{103}Pd production is reactor irradiation of isotopically enriched ^{102}Pd . The low natural isotopic abundance of ^{102}Pd (1.02%) requires the use of moderate to highly enriched ^{102}Pd target material of no less than 50%. Moreover, the low cross-section of $^{102}\text{Pd} (n,\gamma) ^{103}\text{Pd}$ nuclear reaction (thermal cross-section is 3.4 barn, resonance

integral 10 barn) requires also the use of highflux nuclear reactors, like the HFIR (ORNL, Oak-Ridge, USA) or SM (RIAR, Dimitrovgrad, Russia), to produce high-specific activity ^{103}Pd . Unfortunately, the enrichment of palladium with ^{102}Pd rarely exceeds 50-80%, i.e. this material contains other palladium isotopes, like ^{108}Pd and ^{110}Pd . These isotopes can be activated by neutron irradiation, for example ^{108}Pd produces ^{109}Pd ($T_{1/2}= 14$ h) that cannot be separated from ^{103}Pd by chemical means (IAEA, 2006; Levin 1969; Tarapcik and Mikulaj, 1969).

Under the Co-ordinated research project (CRP), methods for the production of ^{103}Pd and seed cores of palladium have been developed by the Russian Federation participant. An approach based on nuclear reactor irradiation of isotopically enriched ^{102}Pd (up to 80%) has been tested for ^{103}Pd production (IAEA, 2006).

Irradiation in the high-flux reactor (neutron flux density higher than $1 \times 10^{15} \text{cm}^{-2} \text{s}^{-1}$) provides palladium-103 with specific activity up to approximately 500 Ci/g ($1.85 \times 10^4 \text{GBq/g}$).

Based on this result, it can be envisaged that moderate flux reactors with neutron flux density of $10^{14} \text{cm}^{-2} \text{s}^{-1}$ can be also used for ^{103}Pd production with specific activities much higher than the required minimum of 5 Ci/g ($1.85 \times 10^2 \text{GBq/g}$) for brachytherapy seed production.

^{103}Pd decays by electron capture and emits characteristic x-rays of 20.1 keV (0.656/dis) and 23.0 keV (0.125/dis) (Figure 2.2) (Yu et al, 1999). The half value layer in lead is 0.008 mm. Having a shorter half-life (17 days) than that of ^{125}I (59.4 days), ^{103}Pd may

provide a biologic advantage in permanent implants because the dose is delivered at a much faster rate (Khan, 2003).

The active radionuclide is plated onto two graphite pellets on either side of a lead radiographic marker within the titanium capsule and each end of the seed is cupped inward i.e. it is concave (Yu et al, 1999). Absorption of incident photons by the titanium wall and lead marker, and the self shielding by palladium result in an anisotropic emission pattern with an axial fluence much lower than the fluence along the transverse axis (Chiu-Tsao and Anderson, 1991). This is a salient feature of the ^{103}Pd seeds and therefore can be used to uniquely identify ^{103}Pd seeds.

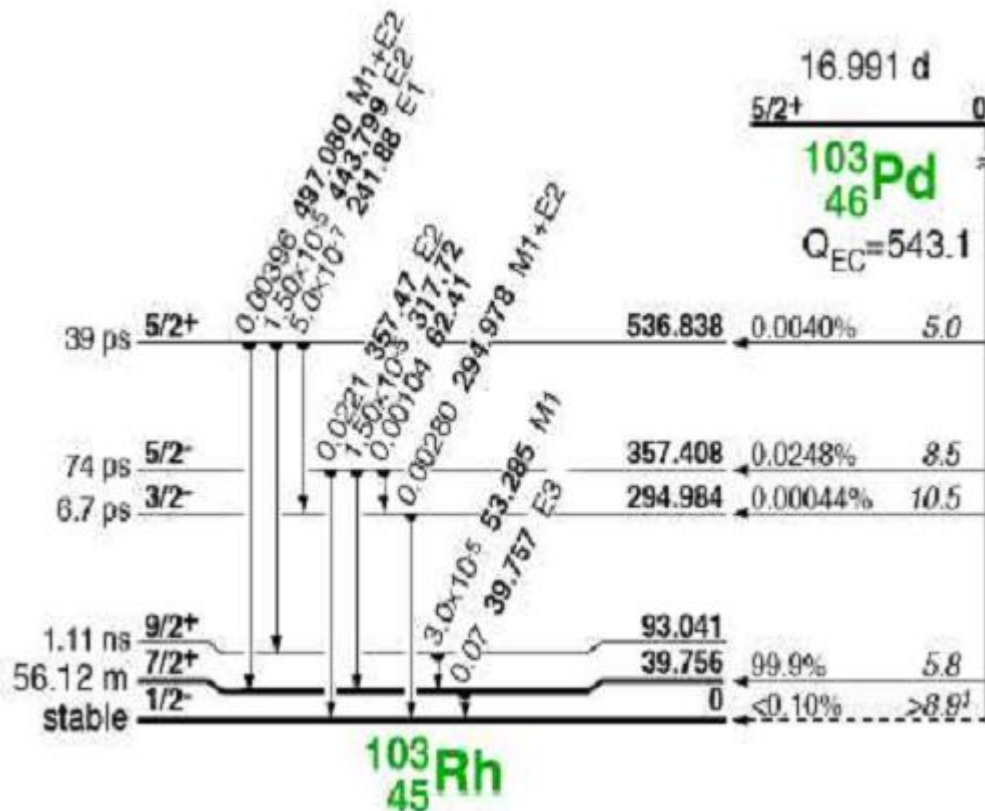


Figure 2.2: Pd-103 decay diagram.

2.2.1.2 Transrectal ultrasound prostate brachytherapy

In the 1980s, several investigators were exploring new brachytherapy approaches to the treatment of prostate cancer. Martinez treated patients with EBRT combined with temporary seeds inserted using a transperineal approach. Drs. Syed and Puthawala pioneered a temporary seed technique of placing the needles while visualizing them through an open laparotomy. In 1983, Dr. Holm introduced the use of transrectal ultrasound to visualize the permanent placement of I-125 seeds via needles inserted through the perineum directly into the prostate. The procedure consists of using a transrectal ultrasound probe to first define the prostate contours in 5mm thick transaxial images for dosimetric planning and then, some weeks later, delivering radioactive seeds into the prostate gland. In both steps, the patients are placed in lithotomy position. Needles containing the seeds are inserted through the perineum into the prostate under the guidance of transrectal ultrasound probe. The needles are prepared for the procedure in one of three ways: manual loading on site, purchased pre-loaded needles and seed loading device (CAPCA, 2007). The ultrasound-guided transperineal approach resulted in relatively even distribution of seeds throughout the prostate; this marked a major advance in prostate brachytherapy in that it minimized the need for external beam radiation and allowed more precise planning of the implant prior to the procedure (Grimm et al, 2001). These advances also significantly increased the accuracy of seed placement and ensured that the prostate would receive the proper number, strength, and positioning of radioactive sources. Derivatives of this technique are in wide use today.

The first transrectal ultrasound-guided, template-guided I-125 implant procedure was performed at the Seattle Prostate Institute in late 1985 and is now being used in over 600 centers around the world. The original Seattle approach has been modified and improved several times since the original implants.

Today, the implant is planned prior to the procedure either on the day of or several weeks prior to the implant. Typically, the implant is completed in a 45-90 minute outpatient procedure under spinal anesthesia or light general anesthesia (Grimm et al, 2001).

2.2.1.2.1 Transrectal ultrasound system (TRUS)

The transrectal ultrasound system includes the ultrasound machine, the rectal probe, the stepping device/probe carrier, the perineal template, and the stabilizing mechanism. The ultrasound machine is typically a portable unit, and contains a seed implant software package such that a grid pattern can be displayed on the screen. The stepping device allows the rectal probe to be attached to the stabilizing mechanism while permitting movement in and out of the patient's rectum in precise steps. The needle template has holes accepting 17 gauge or 18 gauge needles, arranged typically in a 13 by 13 matrix, at 5mm spacing. The template may be designed to mount directly to the rectal probe in some commercial systems, in which case it moves together with the probe, or it may be mounted on the probe carrier, in which case it remains stationary with respect to the perineum as the probe is moved. In either case, the holes on the needle template correspond to the grid points displayed on the TRUS monitor screen. The stabilizing mechanism immobilizes the entire rectal probe/carrier/template system against the

operating table or floor, to prevent unintentional motion of the probe and needle template during the implant procedure. The template is placed at close proximity to the perineum to minimize needle splaying in the target volume.

2.2.2 The HDR brachytherapy system.

High dose rate brachytherapy is an established and rapidly advancing technique used to deliver highly conformal doses of radiation in the treatment of prostate cancer (Badiozamani et al., 2005). Remote afterloading device, a type of HDR brachytherapy system using high activity iridium 192 sources are commonly used in a variety of centers throughout the world.

2.2.2.1 Radionuclides used in HDR brachytherapy systems.

HDR brachytherapy uses a single radioactive seed made of iridium-192 which is sometimes referred to as an iridium wire. Soft flexible plastic catheters are inserted through the perineum and into the prostate gland.

2.2.2.1.1 Iridium -192

Iridium-192 has a half- life of 73.8 days and emits gamma photons with energies ranging from 9keV to 884.5keV (figure 2.3), but the weighted average energy of an iridium- 192 brachytherapy source is 397keV (Goetsch et al, 1991). With a high maximum- activity concentration of 330GBqmm^{-3} , iridium-192 is suitable for high-activity afterloading

sources; it is also available in the form of seeds and flexible wires. In wire form it is produced by reactor irradiation of a 75 % / 25 % iridium / platinum alloy, which is usually provided as a wire, clad with 0.1mm of pure platinum. The iridium / platinum wire is available with 0.3mm and 0.6mm overall diameter. There are two types of iridium-192 seed sources available commercially, both having a physical length of about 3mm, the primary difference being that of encapsulation.

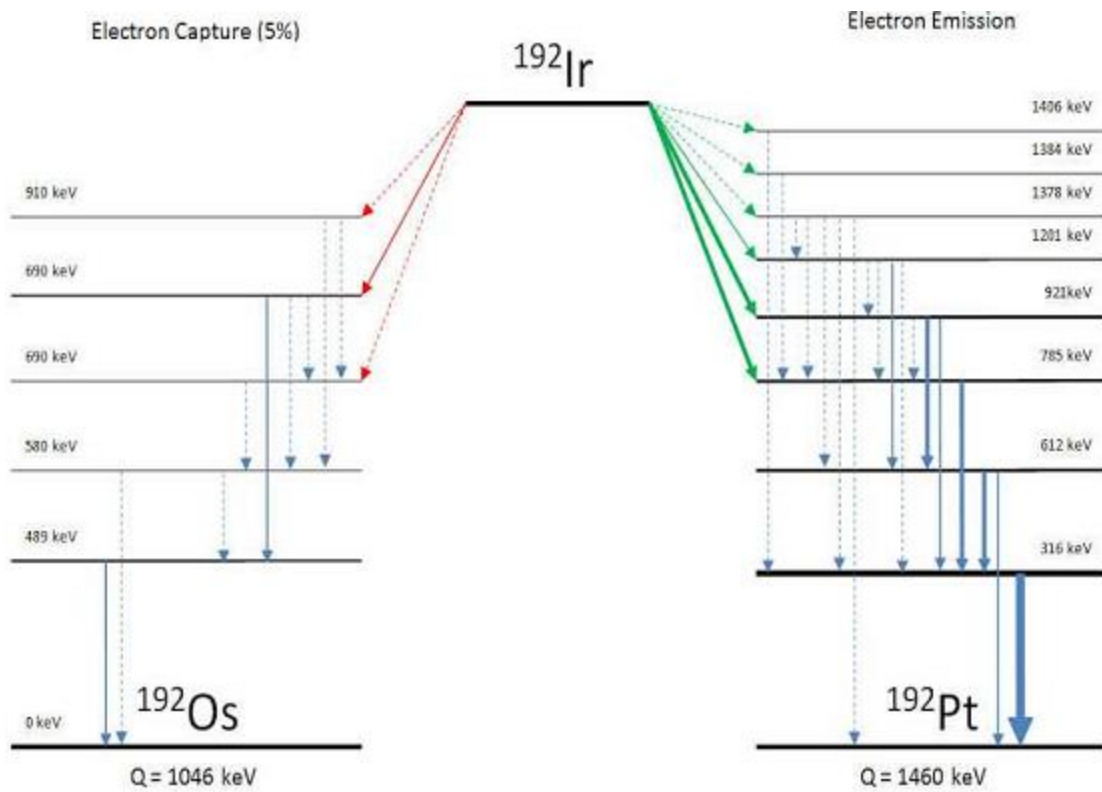


Figure 2.3: Ir-192 decay scheme

2.2.2.2 Afterloading system

Brachytherapy sources are usually inserted into catheters or applicators. One of the major exceptions to this is prostate seed brachytherapy, where sources are placed directly into the tissue of the prostate. When the radioactive brachytherapy source is positioned in the

patient after the surgical procedures, i.e., after the insertion of the applicators, the technique is called “afterloading”. Then, the time that it takes to place the applicators in the pre-determined position is not a problem in terms of staff irradiation, because the applicators are positioned without sources inside them. Afterloading for brachytherapy was introduced in order to reduce the radiation dose to some radiotherapy staff groups, such as the radiotherapist performing the brachytherapy and the theatre staff attending the insertion. The early steps in afterloading techniques were developed by many distinguished investigators (e.g., Tudway, 1953; Henschke, 1960; Suit et al 1963; Ridings, 1963; Horwitz et al 1964), and the exposure reduction due to the use of these techniques is well documented in many papers like Suit et al 1963, Haybittle and Mitchell 1975, Redpath and Douglas, 1976. The two types of afterloading techniques are manual and remotely controlled. The first methods used manual afterloading, in which the inactive applicators or needles were positioned and checked before the active sources were introduced. With the advent of remote afterloading techniques, the radiation dose to other staff, such as nurses, source curators and technical staff preparing radionuclide source train was reduced.

2.3 Acceptance testing, commissioning and quality control of LDR prostate brachytherapy systems.

Low dose rate prostate brachytherapy equipment that is newly acquired or substantially upgraded requires acceptance testing before being put into clinical service. Acceptance testing and commissioning have several purposes:

- To ensure that the stated specifications or equipment and performance are achievable,
- To establish baseline parameters for the future quality control program,
- To familiarize the customer with operation of the unit.

2.3.1 Acceptance testing of LDR prostate brachytherapy system

In addition, acceptance testing of the equipment and facility will include establishing compliance with applicable radiation safety codes. These are included in the ultrasound federal and/or provincial or national regulations and it is the supervising physicist or qualified expert's responsibility to be familiar with these requirements and to demonstrate compliance.

Decommissioning of radiotherapy equipment and facilities may also be regulated by provincial and/or federal authorities. All imaging modalities and treatment planning systems that are used in prostate brachytherapy and those that are newly acquired or substantially upgraded require acceptance testing before being put into clinical service. Acceptance tests are customarily described in a document prepared by the vendor, although the purchaser may wish to specify additional tests. The document is signed by the purchaser upon satisfactory completion of testing, before which formal purchase of the unit should not be completed. The dosimetric description of the sources should be made according to AAPM Task Group 43 recommendations (Nath 1995, Rivard 2004). The AAPM and the Radiological Physics Center (RPC) jointly maintain a registry of low-energy brachytherapy seed designs that meet the AAPM dosimetric prerequisites. Any new or upgraded

treatment planning system and / or new seed model should be validated against known test cases and also by hand calculation. Before using a seed model clinically for the first time, a well chamber should be sent to an accredited dosimetry calibration laboratory (ADCL) for calibration. Alternatively, a single seed can be sent to an ADCL for measurement of its air kerma strength, and this value used to obtain a calibration factor for the well chamber. Compliance with applicable radiation safety codes must be ensured for each radionuclide, source type and activity range to be used. The standards for acceptance testing of prostate brachytherapy systems should be consistent with the routine quality control objectives and criteria applied subsequently. As such, the system should meet or exceed the specified tolerance levels.

Tests on all functional systems and sub-systems of the equipment must be included. These tests should be performed by, or under the supervision of, a qualified medical physicist. Adherence to these standards provided by the manufacturer must be demonstrated and documented, in or outside of the vendor's acceptance testing protocol, before a new LDR prostate brachytherapy system or major upgrade is accepted, and put into clinical service. Also, an appropriate subset of acceptance tests must be performed after any repair or preventive maintenance interventions on the equipment. The extent of testing required must be judged by a qualified medical physicist, and must include any items that may have an impact on the performance and accuracy of the prostate brachytherapy program.

2.3.2 Commissioning of LDR prostate brachytherapy system

Commissioning generally refers to the acquisition of additional measured data from a unit after most acceptance testing is completed, with two purposes:

- To acquire data required for dose calculation and for the treatment planning process,
- To establish additional baseline parameters for the future quality control program.

The specific commissioning measurements required will depend on the prostate brachytherapy equipment, program and technique that are adopted. The manufacturer usually makes recommendations on system specific commissioning measurements but the physicist can refer to sources in the literature as well. The resulting data should be compiled into a commissioning document that would allow future physicists the ability to compare their own measured data with the initial commissioning set. It is essential to recognize that commissioning prostate brachytherapy techniques involves more than just ensuring that the equipment itself works properly. The whole treatment chain, including the measuring, imaging modalities and treatment planning system must be tested in addition to the delivery unit and the brachytherapy tools. Clearly all the tests necessary must be performed at acceptance and commissioning time with the intended local test equipment and protocols if meaningful baselines are to be established. Decommissioning of radiotherapy equipment and facilities may also be regulated by provincial and/or federal Regulatory authorities.

2.3.3 Quality control of LDR prostate brachytherapy system.

According to ISO 9000 (ISO 2000), quality control is “the part of quality management focused on fulfilling quality requirements”. Quality as defined by (ISO 2000) is “the degree to which a set of inherent characteristics fulfils requirements.” In brachytherapy parameters controlled in daily or weekly tests are such inherent characteristics.

Requirement is “the need or expectation that is stated, generally implied or obligatory.” The requirements are stated in standards, by authorities or in local procedures taken from recommendations.

The purpose of a quality control program is to assure that operational standards for a unit that were considered acceptable at time of purchase continue to be maintained, as closely as possible, over the life of the unit. Thus, quality control tests typically are periodic repetitions, partial or full, of acceptance and commissioning tests. For LDR prostate brachytherapy, tests are required for mechanical, radiological and safety systems.

2.4 Treatment planning and dosimetry of LDR prostate brachytherapy systems.

2.4.1 Interstitial implants

An interstitial implant administers a high dose of radiation to the tumour, whilst effectively sparing surrounding normal tissues and nearby critical organs. The dose homogeneity of such implant will be different from that achievable with external beam radiotherapy, as there is a very high dose region immediately around the implanted sources. This high dose region is within the target volume and is not clinically significant.

In order to ensure adequate tumour coverage and sparing of critical organs, dosimetry systems are usually based on the minimum dose to a volume.

In the 1930s (Paterson and Parker ,1934, 1938) developed the Manchester system and Edith Quimby developed the Quimby system (Quimby and Castro 1953, Goodwin et al., 1970) for use with radium sources. These two systems had their own unique implantation rules and dose specification, but were completely self-consistent and have been used for many years to calculate dose to tissue. Dosimetry systems have been developed for interstitial treatments to ensure reproducibility between implants and adequate coverage of tumour volumes, provided that the rules that have been developed are adhered to as closely as possible. Once other isotopes became available, other implantation systems with their own implantation rules were developed.

2.4.2 Postimplant dosimetry

Prostate implants are generally planned to deliver a prescribed minimum dose. However, it has been shown that the minimum dose planned can rarely be achieved due to seed placement errors which are inherent in the procedure (Yu et al, 1996; Roberson et al, 1997, Roy et al, 1996 and Yu et al, 1999). Furthermore, postimplant edema can further reduce the dose delivered by the implant (Waterman et al, 1997; Waterman et al, 1998; Prestidge et al, 1998). Hence it cannot be assumed that the patient would receive the dose prescribed in the pretreatment dosimetric plan. Postimplant dosimetric evaluation was traditionally carried out using multiple radiographs. Although such plane films are adequate for reconstruction of the relative seed positions, they cannot provide the dose

delivered to the prostate because the prostate cannot be visualized on a radiograph. Postimplant dosimetry was limited to a calculation of the matched peripheral dose (MPD), a parameter that has been shown to be an unreliable indicator of the dose delivered to the prostate (Roy et al, 1993; Yu et al, 1999). The dose delivered to the prostate and other organs can be determined by performing a postimplant CT-based dosimetric analysis. The advantage of CT-based dosimetry is that the prostate and other organs, such as the rectum, can be visualized and also CT images of the pelvis provide excellent source definition within the limits of axial slice spacing and partial- volume artifact, and exhibit reasonable soft- tissue contrast. This capability allows dose-volume histograms (DVHs) to be generated, which provide detailed information on dose coverage and implant quality. At present, a postimplant CT study is the most direct method for carrying out quantitative dosimetric evaluation. CT-based dosimetric evaluation is particularly important during the early stages of a new prostate seed implant program to aid the team in progressing up the learning curve as quickly as possible. Continuous evaluation of implant quality permits improvement in techniques as the program develops. Otherwise, problems which compromise implant quality may go undetected and be perpetuated indefinitely.

2.4.3 Computerised dosimetry.

Dose computations algorithms have evolved over the years to calculate dose distributions around source in a variety of planes and orientations. Stovall and Shalek (1972) and Shalek and Stovall (1975) described a number of computer techniques available at that time. These have since been extended to include the calculation of source coordinate

from radiographs, and the sorting of multiple seeds and wires particularly useful for prostate implants.

Welsh et al. (1983) have reported that with their computer dosimetry system, repetition of the dose distribution calculation for the same wire arrangement may show differences of as much as 5% in the dose at individual points although the average discrepancy is much less than this (<3%).

To verify computer calculations a database of individually measured data or appropriate published data must be available. For external beam treatments, data are already measured for individual linear accelerator to be used. However, brachytherapy is different in that experimental determination of dose rates, at short clinically relevant distances around brachytherapy sources are extremely difficult and there can be large uncertainties in the measurements. Several phantoms have been developed to check consistency of dose distribution but absolute dosimetry is one of the problems. Some errors in computer dosimetry have been found to be because of incorrect input parameters, particularly the use of incorrect exposure rate constant or unit of source strength. For a particular brachytherapy computer planning system users are constrained by the concepts in the software development as well as the validity of the calculation algorithms (IAEA, 2004; ESTRO, 2004). It is important to apply a source calibration methodology that is consistent with the assumptions made by the software designer.

2.4.4 Treatment planning system.

Computerized treatment planning plays an important role in modern prostate brachytherapy. Careful dosimetric planning leads to smooth and expedient implantation, and reduces the likelihood or extent of normal tissue radiation damage. The process of dosimetric planning is especially helpful to the implant team in the early stages of implementing the prostate brachytherapy program. A treatment-planning system specifically designed for prostate gland implants allows the target outlines from the volume study to be digitized into the computer. The implant is planned with an inter-seed spacing of 1 cm (center to center) and a needle spacing of 1 cm. The VariSeed software (Varian medical services) allows placement of seeds in the template grid in each of the ultrasound images. The software also helps provide dynamic dosimetry to update the dose map in real time as the individual seeds are deposited in the prostate or being added and deleted iteratively to optimize isodose coverage of the target volume (Varian medical services, 2006), the prowess panther software also allows a planning for brachytherapy cases including permanent seed implants. Before the availability of computer dosimetry, seed strength and the required number of seeds were determined by the method of dimension averaging used in conjunction with a pre-calculated nomogram. The modern computer programs allow the use of any seed strength as well as fine adjustment of this parameter to obtain the desired MPD. Typical seed strengths required are on the order of 0.3 mCi for ^{125}I (MPD = 144Gy) and 1.7 mCi for ^{103}Pd (MPD = 125Gy) (Khan, 2003). Based on the approved computer plan, a worksheet is prepared specifying the number of needles, seeds in each needle and the template co-ordinate.

2.4.5 AAPM TG-43 formalism

Dose calculations are presented in this study for photon emitting sources only. The dose calculations are divided into two categories: the first is the TG-43 formalism, which can be considered as the most complete formalism today. This approach is used in modern TPSs and is suitable as a method for commissioning and the second category is an independent protocol developed on the centre, it may be used for quick checks and verification of treatment plans.

In 1995 the AAPM TG-43 (Nath et al, 1995) introduced a dose calculation formalism to establish the 2-D dose distribution around cylindrically symmetric sources. It is based on measured quantities such as, dose rate constant, geometry factor, anisotropy function, radial dose function and air kerma strength. Previous calculation formalisms were based upon apparent activity (A_{app}), equivalent mass of radium, exposure-rate constants, and tissue-attenuation coefficients, these older formalisms did not account for source to-source differences in encapsulation or internal construction (Nath et al, 1995). Except for radium, the exposure-rate constants and other input parameters to these algorithms depended only on the radionuclide. This protocol, which was later updated in 2004 by (Rivard et al, 2004), describes a dose calculation formalism that uses new dosimetric functions derived from phantom measurements and Monte Carlo simulation together with realistic source geometry.

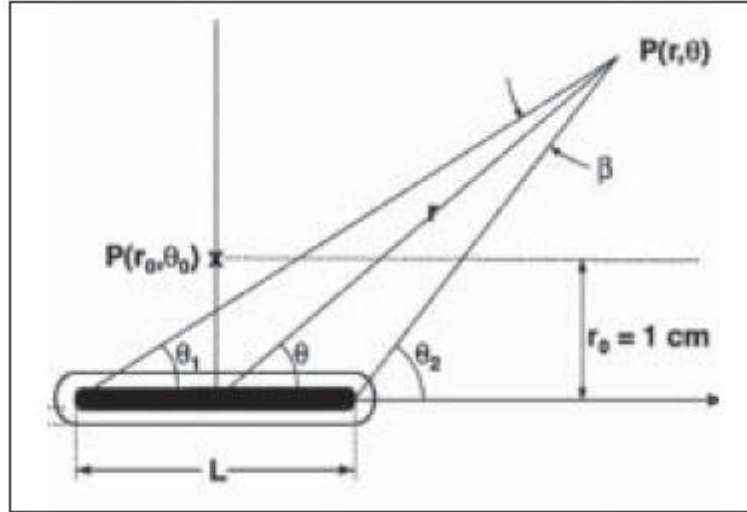


Figure 2.4: Geometry and coordinate definitions used in the TG-43 dosimetry protocol

The quantities used in the calculation of absorbed dose in the TG- 43 Formalism are measured for the specific type of source. This implies that, aside the photon spectrum and medium, the TG- 43 formalism depends on source construction and geometry as well. Figures 2.4 summarizes the geometry and coordinate definitions used in the TG- 43 dosimetry protocol. The origin of the coordinate system is positioned at the centre of the active core of the source and z-axis along the tip of the source. A cylindrical symmetry for the activity distribution within the core is assumed.

TG-43 protocol expresses the dose rate \dot{D} at a point in water with co-ordinates (r, θ) from the center of the source with air kerma strength S_K , as:

$$\dot{D}(r, \theta) = S_K \cdot \Lambda \cdot \frac{G_L(r, \theta)}{G_L(r_0, \theta_0)} \cdot g_L(r) \cdot F(r, \theta) \quad \text{Eq. 1.0}$$

Where:

r = distance from the origin to the point of interest P;

θ = angle between the radius vector r and the long axis of the source;

Λ = the dose rate constant, defined as the dose rate to water at a distance of 1cm on the transverse axis of a unit of air kerma strength source in a water phantom;

S_k = air kerma strength, which is a measure of the brachytherapy source strength, is specified in terms of air kerma rate at a point along the transverse axis of the source in free space (it is defined as the product of air kerma rate at a calibration distance in free space $K(d)$, measured along the transverse bisector of the source, and the square of the distance d):

$$S_k = K(d) \cdot d^2$$

$G(r, \theta)$ = the geometrical function accounts for the variation in relative dose due to only the spatial distribution of activity throughout the source. It does not include the effects of photon absorption and scattering within the source;

The reference point (r_0, θ_0) which lies on the transverse bisector of the source at a distance of 1 cm from its centre i.e. $r_0 = 1\text{cm}$ and $\theta_0 = \pi/2$;

$F(r, \theta)$ = the anisotropy function accounts for angular variation of the dose distribution around the source due to absorption and scattering of photons by the encapsulating material and the surrounding medium; and

$g(r)$ = the radial dose function defines the fall-off of dose rate along the transverse axis due to absorption and scattering in the medium. It is also influenced by filtration of photons by the encapsulation and source materials.

2.4.5.1 Application of TG-43 to I-125 dosimetry

The dosimetry of iodine- 125 has always had a higher degree of uncertainty than that of isotopes emitting higher energy radiation. Difficulties in experimental dosimetry as found in brachytherapy tend to increase in the case of very low gamma energy emitting sources such as iodine-125. The use of the TG-43 data involved a decrease of ten percent in dose calculated at a distance from a seed. This arose mostly from a change in the recommended values for the dose rate constant and the anisotropy factor for the Amersham sources which were almost exclusively used at that time (Kubo et al, 1998; Williamson et al, 1999). In recent years two important changes that affect the iodine-125 dosimetry have been introduced:

- (i) the dosimetry parameters proposed by TG-43 (Nath et al, 1995), and
- (ii) the adoption by The National Institute of Standards and Technology (NIST) of a new primary calibration standard in 1999 (Seltzer et al, 1998). Both imply changes in the dose rate constant, Λ , and can require modifications in the prescribed dose, in order to estimate in a more precise way the delivered dose.

With the improvement in the knowledge of properties of iodine-125 and the measurement instruments and methods, the dosimetry parameters have been continuously reviewed with smaller tolerances on uncertainties. So, in 1995, TG-43 recommended dosimetry

parameters that differed between 10 and 18% from the ones used previously, for the seed models 6711 and 6702. (Bice et al, 1998) showed that in a prostate implant with model 6711 seeds, this modification should lead to changes in prescribed dose from the typical 160 Gy value to a minimum of 144 Gy.

On other hand, from 1 January 1999 the NIST has implemented the new standard for I-125. In the old standard, the measurements were affected by the characteristic X-rays from Ti, which do not contribute to the dose in water at distances beyond 1 mm. The new standard is based upon measurements using a wide-angle free-air chamber with a thin absorber to eliminate these X-rays and other contamination contributions.

To implement the change described by of the NIST99 standard on sources specified with it, it is recommended to modify the dose rate constant value, increasing it with a factor inverse to the reduction of the of \dot{K}_R of the source. So the delivered dose does not change and it is not necessary to change the dose prescription (Kubo et al., 1998b, Williamson et al., 1999).

This modification does not change the delivered dose to the patient because the reduction of \dot{K}_R of the sources is equal to the increased value of Λ . As a consequence, today all seed sources are specified according to NIST99 and the user must be cautious with the implementation of the Λ value. If the dose rate constant is adopted from a dosimetry study from literature that has taken into account the NIST99, its value must be maintained. In the other case the user must modify the original value in a factor inverse to the reduction of the of the seed model with the new standard. For example, for the ^{125}I source models 6711 and 6702 from Amersham, the dosimetry study used from literature

was published on 1995 (Nath et al., 1995), so the value of Λ must be multiplied by 1.115 (Williamson et al., 1999). Rivard et al. provide a set of consistent values. Further refinements of the values for dose rate constant to be used for different source designs have been achieved and the up-to-date recommended values for Λ can be obtained from Rivard et al., 2004.

2.5 Performance evaluation protocols for LDR prostate brachytherapy systems.

Reports on quality control in The Netherlands are published by the Netherlands Commission on Radiation Dosimetry (NCS, Nederlandse Commissie voor Stralingsdosimetrie). In NCS Report No 4 (1989; published in Dutch; an English synopsis was published in 1991: “Recommendations for dosimetry and quality control of radioactive sources used in brachytherapy”) recommendations were given for the specification of the source strength and dosimetry of low dose rate (LDR) sources. The report includes guidelines for calibration of sources as well as for radiation protection.

Furthermore, several articles were published on behalf of the American Brachytherapy Society presenting the recommendations for permanent implant brachytherapy, specifically for the treatment of the prostate (e.g., Nag et al 1997, 1999, 2000; Beyer et al 2000). In general, all these reports are widely spread throughout the world and have a major influence on the establishment of QA program in brachytherapy clinics.

Several important reports were published in the last decade by the AAPM. These reports consist of series of tests to be performed, along with their minimum frequency. The tests

are derived from the published literature and, in particular, the standards laid out in the AAPM documents, TG 43 (Nath 1995), TG-64(Yu 1999) and TG-1(Goodsitt 1998)

A draft ICRU report on the dose specification in interstitial brachytherapy has been prepared and a provisional summary of it has appeared in print. On the basis of information available to date, the reporting parameters therein recommended are closely related to those of the Paris system. Thus reported doses are defined primarily in the central plane as in the Paris system, and the basal dose and the reference have been renamed the mean central dose and the peripheral dose respectively.

The ABS (AES at the time) physics committee, formed in 1986, adopted dose specifications as its first assignment and published society approved recommendations in 1991(Anderson et al, 1991).

CHAPTER THREE

MATERIALS AND METHOD

Chapter three focuses on the experimental framework and the performance evaluation of the transrectal ultrasound system as well as the verification of dose obtained from the treatment planning system.

3.1 Performance evaluation of the transrectal ultrasound system

3.1.1 Materials and equipment

The materials and equipment used for this research include the following;

- i. Brachytherapy QA phantom (CIRS model 045)
- ii. Transrectal ultrasound system (B-K Medical- Falcon 2101 EXL)
 - Rectal probe
 - Template grid and stepper
 - Ultrasound unit
- iii. Gel (Aquasonic ultrasound gel)
- iv. Implant needles (Bard[®] Brachystar[®] , REF 917205, LOT RESDO380)

3.1.1.1 Brachytherapy QA phantom (CIRS model 045)

The model 045 QA phantom was developed by CIRS to provide a reliable tool for quick quality control checks on most prostate brachytherapy ultrasound systems. This phantom

(Plate 3.1) offers a stable medium and contains specific known test objects. The phantom is constructed from zerdine which simulates the acoustical properties of human tissue. It is housed in PVC for added durability.

The CIRS series of ultrasound phantoms, unlike human subjects or random scannable materials, offer a reliable medium which contains specific known test objects for repeatable qualitative assessment of ultrasound scanner performance over time. CIRS is certified to ISO 9001:2008 standards.

The phantom consists of 13 parallel target wires of 0.1 mm diameter, making an N-shape and positioned at 10 mm intervals in both lateral and axial directions. The position of a target wire is defined by a combination of rows (1 – 5) and columns (B – F) (Figure 3.1). Three volumes made of zerdine® with sizes 4 cm³, 9 cm³ and 20 cm³ located in the phantom are used for volume measurement accuracy.

Five cross wires are embedded within the phantom to determine if the probe is being retracted at the specified distance. By turning the probe at an angle of 60° to the right or left, the three calibrated volume objects are visualized, one of which is not spherical.



Plate 3.1: The CIRS Model 045 brachytherapy QA phantom.

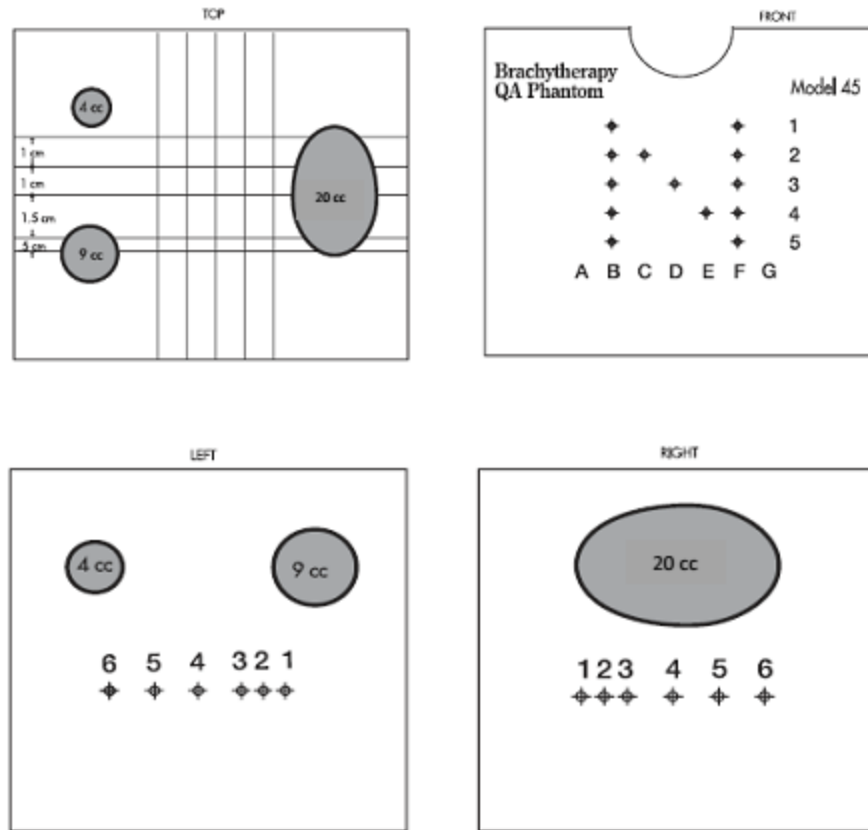


Figure 3.1: The schematic diagram of the QA phantom

3.1.1.2 Transrectal ultrasound system (B-K Medical-Falcon 2101 EXL)

The ultrasound unit (BK Medical Falcon 2101 EXL, USA) used for acquiring ultrasound images in the study is shown in Plate 3.2. The system is connected to a transrectal probe, which is held in position by a stabilization mechanism and its movement controlled by a calibrated stepper. The stepper enables accurate and reproducible positioning of the probe within the rectal canal. The system has multitude of uses with an imaging frequency range from 1 to 16 MHz. The ultrasound machine has a

seed implant software package such that the grid pattern can be displayed on the screen; similarly it displays the sagittal as well as the transverse planes of the prostate volumes. This feature is very helpful in guiding individual needle insertions and visualizing the movement of the prostate volume as the needles are inserted into the volume.



Plate 3.2: The B-K transrectal ultrasound system.

The rectal probe is inserted into the rectal cavity (the scanning surface of the phantom), and images generated from the probe are used to assess the size and shape of the reflective targets in the phantom. The rectal probe is mounted on the stepper to aid in its movement in and out of the phantom. The probe incorporates two orthogonal arrays, one sagittal array for base-apex imaging and a transverse array for imaging of the prostate in the orthogonal plane (Plate 3.3).



Plate 3.3: The rectal probe used in this work.

The needle template has holes which can accept 17 gauge or 18 gauge needles, arranged typically in a 13×13 matrix, at 5 mm spacing (Yu et al, 1999). The template may be designed to mount directly to the rectal probe in some systems, in which case it moves together with the probe, or it may be mounted on the probe carrier, in which it remains stationary with respect to the perineum as the probe is moved, the latter as shown in Plate 3.4 was used in the study.

The template grid should correspond precisely with the electronic grid of the ultrasound machine; the grid is used to guide the needles into the perineal area. The co-ordinates on this grid or template are used to pinpoint the exact positions in the prostate where the seeds should be placed.



Plate 3.4: The template grid.

The stepping device (Plate 3.5) allows the rectal probe to be attached to the stabilizing mechanism while permitting movement in and out of the patient's rectum (scanning surface of the phantom) in precise steps.



Plate 3.5: The stepper with the probe and template holders.

The stabilizing mechanism (Plate 3.6) immobilizes the rectal probe and template system against the operating table or floor, to prevent unintentional motion of the probe and needle template during the implant procedure.

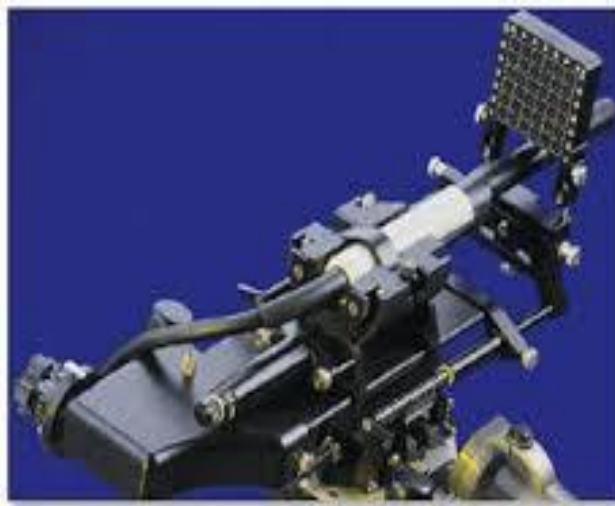


Plate 3.6: The stepper, probe and template mounted on the stabilizing mechanism.

3.1.1.3 Gel

When the particles of the medium move in response to an ultrasonic wave, there is a particle velocity associated with this movement. Oscillation of particle velocity, v , and acoustic pressure, P , in a plane progressive wave are in phase: that is the particles move fastest when the acoustic pressure is greatest. P and v are also proportional, and the constant of proportionality P/v is called the specific acoustic impedance, Z . Changes in specific acoustic impedance control transmission and reflection at interfaces. When a very large proportion of the ultrasound energy incident upon a boundary is reflected, the residual intensity becomes too low for interrogation of structures lying beyond the boundary. Ultrasound gel is a conductive medium that is used in ultrasound diagnostic techniques and treatment therapies because the gel reduces reflections at the boundary. It is therefore necessary to apply suitable gel or oil between the transducer surface and the patient's skin in order to remove air and also help conduct sound waves from the transducer into the patient's body. In the case of this study, the gel was applied to the scanning surface of the phantom.

3.1.1.4 Implant needles

The needle has ergonomic stylet hub, etched cannula tip and enhanced needle design for a stiffer cannula and better trackability for placement of radioactive seeds in the prostate gland. It has a lubricious coating and cm markings with dimensions of 17g mass and 20cm length.

Each needle as shown in Plate 3.7 is fixed on the template grid with holes on either side, to allow the seeds to be deposited in the patient's prostate. The needles used in this study were supplied from the Bard- Company, USA.

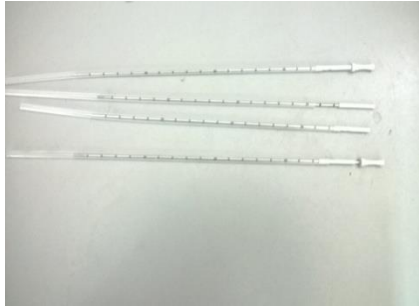


Plate 3.7: The implant needles used in this work

3.1.2 Performance evaluation tests

For all tests conducted, a non-sterile (2 x 14 cm) endocavity balloon was put around the probe to reproduce clinical settings and coupling gel smeared on scanning surface to reduce reflections and artifacts from air bubbles. All tests were performed in accordance with the American Association of Physicists in Medicine (AAPM) Task Group (TG) 128 report on quality assurance tests for prostate brachytherapy ultrasound systems , NCRP, Quality Assurance for Diagnostic Imaging, NCRP report number 99, AIUM technical standards committee on quality control manual for gray scale ultrasound scanners, AAPM TG 1, Real time B-mode quality control test procedures and CAPCA(Canadian Association of Provincial Cancer Agencies), Standard for quality control at Canadian radiation treatment centres.

Images were recorded to document the measurements made to aid reproducibility and also serve as reference points.

A. “N” Target group

The “N” Group is useful for many different measurements. This target group (Plate 3.9) assesses the depth of penetration, vertical distance calibration, horizontal distance calibration, and display grid accuracy. The target group consists of a group of 0.10 mm diameter parallel wires positioned at 10 mm spacing and shaped like the letter “N”. Setup for these measurements is shown in Plate 3.8.



Plate 3.8: The setup for performance evaluation measurements

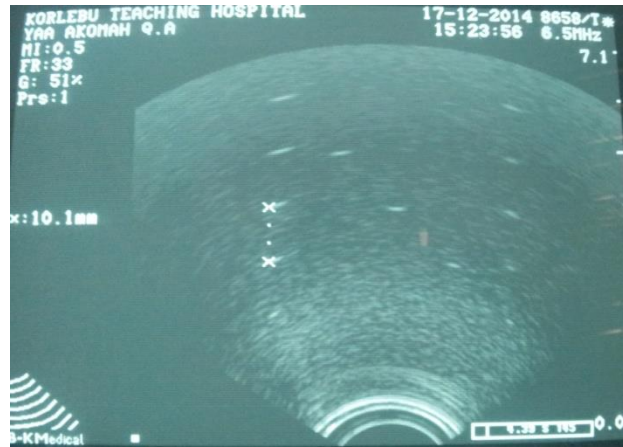


Plate 3.9: The ultrasound image showing the “N” target group.

A.1 lateral and axial distance measurements

Distance measurements in the axial and lateral directions are of importance in making accurate measurements during a procedure, such as to determine the distance of a needle from another needle or from the rectal wall in the x-y axis.

The scan parameters were set consistent with clinically used parameters and the probe held in position on the phantom. Once the image of the N-shaped targets were observed on the ultrasound as shown in Plate 3.9, the image was frozen, and distances between the targets in the axial and lateral directions measured with an electronic caliper. This was done at every step (0.5cm) moved between 0.5 - 10.5 cm distance on the phantom. All measurements were repeated two times and recorded. The averages were calculated with the deviations and compared with the tolerances in the set of protocols used (Table 4.1 and Table 4.2).

A.2 Internal grid / template grid alignment

The electronic grid generated by the ultrasound system, provides a reference for needle locations in the treatment plan. For preplanned procedures, it is important to verify that the electronic grid overlay matches the location of the actual needle template. If this alignment is not correct, the needle cannot be physically inserted according to the pre-plan, requiring intra-operative corrections to the pre-plan.

The scan parameters were set consistent with clinically used parameters and the probe was held in position on the phantom. It was then ensured that a location of the maximized “N” target group was obtained after which the internal grid in the ultrasound system was activated. The alignment of the internal grid and the “N” shape target was assessed and deviations measured and recorded.

With the physical template alignment, the phantom was not used; instead a bucket of water of temperature 48 degree Celsius (to obtain sound speed of 1540m/s (N. Bilaniuk and G. S. K. Wong, 1996)) was used (Plate 3.10). In this case the template grid was mounted on the stepping mechanism, above the bucket of water. The implant needles were inserted into selected holes on the template and imaged. The locations of the needle flashes in the image were verified with that of the implant needles on the template grid. Deviations from original holes were measured (Table 4.6).



Plate 3.10: The set up for the template grid alignment test.

A.3 Lateral and axial resolution test

While ultrasound guidance of prostate implants does not depend as critically on spatial resolution as do most diagnostic studies, certain aspects of the procedure can place a demand on the resolution of the system (Pfeiffer et al, 2008). Poor resolution will make it difficult to properly identify and locate implanted seeds, or image of the needle may be too spread out to accurately register its location.

In this test, the probe was positioned at a region of the phantom where the targets were maximized. The ultrasound image obtained was frozen and dimensions of the targets were measured axially and laterally with an electronic caliper. Their averages were calculated and deviations were recorded. (Table 4.5)

A.4 Depth of penetration (sensitivity)

This test measures the sensitivity of the system, which determines how deep into the patient a low contrast object can be reliably visualized (Pfeiffer et al, 2008). Any change in the signal to noise ratio SNR will impact this measurement.

Also, with this test, the scan parameters were set consistent with clinically used parameters and the probe was held in position on the phantom. A location in the phantom relatively clear of highly reflective targets was found. With a probe frequency of 6.5MHz, the maximum depth of the ultrasound speckle pattern of the phantom clearly distinguished from the dynamic electronic noise and image frozen. With the help of the electronic calipers, the depth was measured. This was repeated four times to reduce errors since set tolerances were not available. Its average was computed. (Table 4.4)

B. Volume targets

Particularly important for real time dosimetry is the ability of the system to accurately determine the volume of a target. This test requires both a phantom with a three dimensional target of known size and the stepper used during clinical procedures. The phantom, CIRS model 045 contains three different calibrated test objects specifically designed to assess volume measurement accuracy. During the procedure, the probe was turned 60 degrees clockwise and anticlockwise in order to make the images of the volume targets visible on the ultrasound screen.

The images of the volume targets were then contoured using the contouring tool on the ultrasound machine's console from the apex to the base and values obtained were

recorded. This was repeated two times and values recorded. The averages were measured as well as the deviations and compared with the tolerances of the protocols used. (Table 4.3)

C. Cross axis group

Just as vertical and horizontal distance measurements are important for accurate seed placement in the x-axis and y-axis, the condition of the stepping mechanism is critical to accurate seed placement in the z-axis (Pfeiffer et al, 2008). Perpendicular to the “N” target group are five wires all at the same distance from the transducer and which can be found at the side of the phantom, but separated by 5mm and 10mm in the z-axis. This group is used to ensure that the stepping mechanism is retracted by the correct distance.

In this particular test, the ultrasound scanner was switched to the transverse mode. This is because the cross axis group can be viewed in the z direction only. The probe was well aligned and inserted towards the back of the scanning cavity, aligned with the cross wire #6 (Figure 3.1 left) and the stepping mechanism secured in place. At a retraction of 10mm steps (two clicks) into the phantom, the next target was seen and recorded. This was done till the last target was seen (6 targets in all) and the number of clicks were compared to the distances between the targets.

3.2 Dose verification tests.

For the purpose of this work, the dose verification test verifies the treatment dose generated by the treatment planning system and that of the dosimeter used.

3.2.1 Materials and equipment

The materials and equipment used in this part of the work include the following;

- i. I- 125 seed source (Bard BrachySource, model STM 1251)
- ii. “Well type” ionization chamber (HDR 1000 Plus well chamber) and electrometer (MAX 4000)
- iii. Gafchromic EBT2-1417 film (Lot number: 08221302)
- iv. Perspex prostate phantom (17.5 x 14 x 21.5 cm³ perspex)
- v. Prowess panther (v 4.5)
- vi. ImageJ software (IJ 1.48v)

3.2.1.1 I- 125 seed source

The I-125 seed source used for this study was the Bard BrachySource seed implants, sterile with model number STM1251. This kind of seed implants is offered loose (Plate 3.11a), in preloaded configurations, in cartridges (Plate 3.11b) and in separate screw-cap vials (Plate 3.11c) and provided sterile. The BrachySource seed implants consist of a welded titanium capsule containing Iodine-125 adsorbed onto a nickel/copper coated, gold cored aluminum wire.



(a)

(b)

(c)

Plate 3.11a, b, c: Pictures of the loose seeds, seed cartridge and screw-cap vial respectively.

Clinical efficacy of the seeds derives solely from the interaction of the emitted ionizing radiation from the BrachySource seed implants with the tissue being treated. Titanium encapsulation provides good biocompatibility. Total photon transmission is approximately 59% after accounting for attenuation by the titanium capsule and the radio-opaque solid substrate (Bard brachytherapy, Inc). The dose distribution around BrachySource seed implants used is moderately anisotropic (Ling et al, 1983, Ling et al, 1985, Ling et al, 1979). The BrachySource seed implants used in this work have passed leak tests per ISO Technical Report 4826, Sealed Radioactive Sources – Leak Check Methods, showing $< 0.005 \mu\text{Ci}$ (0.19 kBq) of removable I-125, as required by 32III. Adm. Code, Sec. 340.410. The seeds used in this work were left overs from the seeds ordered for patients undergoing permanent prostate implants at the National Centre for Radiotherapy and Nuclear Medicine, Korle Bu Teaching Hospital.

3.2.1.2 Gafchromic EBT2 1417 film

The Gafchromic EBT2 dosimetry film 1417 is a self-developing radiochromic film that does not require chemical/physical processing. Gafchromic® EBT2 is made by combining a clear, polyester over-laminate with the active film coating. The substrate of the active film is a clear 700 gauge (175 micron) polyester. The substrate is coated with an active layer of film, nominally 28 microns thick. The over-laminate, 200 gauge (50 micron) polyester with approximately 25 microns of pressure-sensitive adhesive, is bonded to the coated side of the active film, hence the total film thickness is about 285microns (Andres et al, 2010 and ISP, 2010). According to the manufacturer, the photon response of EBT2 film is nearly energy independent from 50 keV to MV range, which clearly includes energies emitted by LDR I-125 source (Uniyal et al, 2012). The film has an improved uniformity and high sensitivity which can be used in the dose range of 1 cGy - 10 Gy in the red channel and even wider dose range up to 40 Gy in the green color channel. The most attractive features of the EBT2 film to be used for LDR brachytherapy are its high spatial resolution required to assess doses in steep gradient regions about the source, its overall effective atomic number (Z_{eff}) is 6.8 , which makes it near tissue equivalent (Z_{eff} of tissue 6.5) (Uniyal et al, 2012).

3.2.1.3 Perspex prostate phantom

The dose measurements were carried out in a specially designed and locally fabricated perspex prostate phantom. Perspex was chosen as the phantom material because of its local availability, low cost and ease of machining. In addition, it is tissue equivalent ($Z_{\text{eff}} = 6.5$) and also almost equivalent to the gafchromic EBT2 film ($Z_{\text{eff}} = 6.8$), the dosimeter

used in this work. The phantom was designed to simulate the prostate of a patient undergoing permanent prostate seed implantation. The phantom, a cuboid of dimensions $17.5 \times 14.5 \times 21.5 \text{ cm}^3$, comprising of various slabs of 0.5 cm thickness perspex was used for this work.

Twelve holes, 0.1cm in diameter for a model 6711 I-125 seed (diameter 0.8 mm, total length 4.5 mm, active length 3 mm) were drilled on four of the 0.5 cm thick perspex slabs and each one glued unto another undrilled 0.5 cm thick perspex slab with the aid of chloroform. A 5cm thick perspex was attached to both sides of the phantom for radiation protection purposes. Additionally a 0.5 cm thick perspex slab was fixed in between the four drilled perspex slab (two at each side) to house the gafchromic film. Plate 3.12 shows a picture of the phantom. For convenience, the simulated prostate was assumed as a cuboid, although the real prostate is pear shaped.



Plate 3.12: The Perspex prostate phantom

3.2.1.4 Prowess panther (v 4.5)

The prowess panther application software is a treatment planning package for both external and brachytherapy treatments. The software package allows one to carry out planning evaluation of permanent implant prostate cancer treatment. Plate 3.13 shows a picture of the user interface of the Prowess panther software.

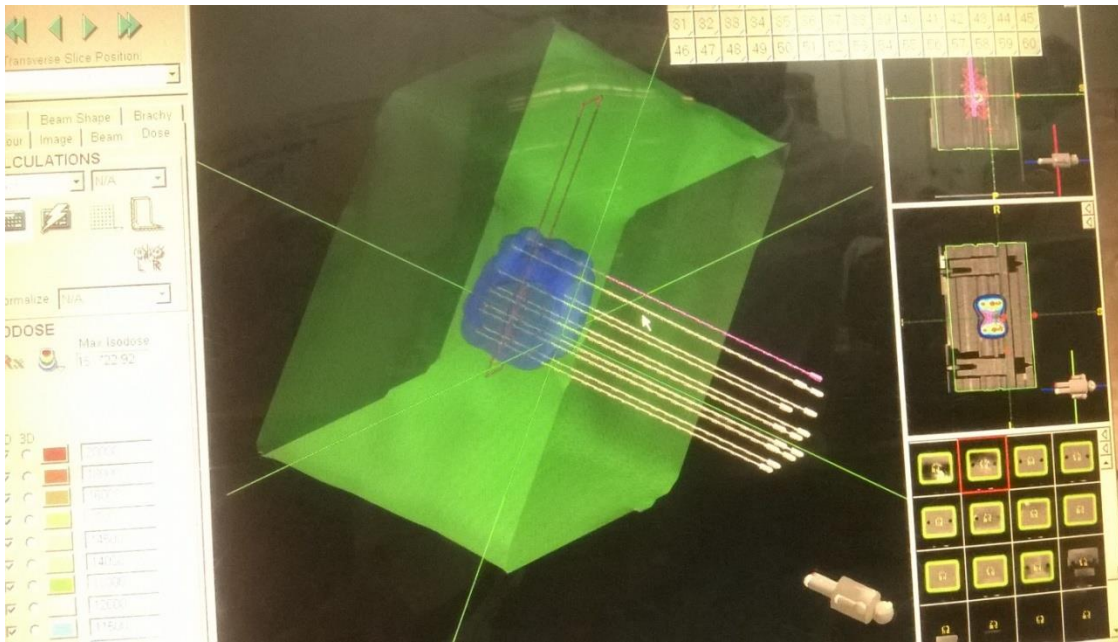


Plate 3.13: The user interface of the prowess panther.

3.2.1.5 ImageJ software

ImageJ is a Java-based image processing program developed at the National Institutes of Health (NIH) (Collins, 2007). ImageJ was designed with an open architecture that provides extensibility via Java plugins and recordable macros (Vijayalakshima and Girish, 2004). User-written plugins make it possible to solve many image processing and analysis problems (Elicieri and Rueden, 2005). ImageJ's plugin architecture and built in

development environment has made it a popular platform (Burger and Burge, 2007, Dougherty, 2005) and therefore was employed for analyzing the optical density of the scanned films in this study. Plate 3.14 shows the ImageJ software interface.

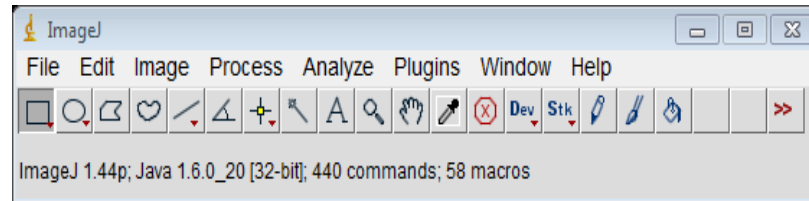


Plate 3.14: An opened view of ImageJ user interface.

3.2.1.6 Ionization chamber (HDR 1000 Plus well chamber) and electrometer (MAX 4000)

The well type chamber for brachytherapy source calibrations is a type designed especially for radiotherapy applications and preferably capable of measuring the reference air kerma rate of both LDR and HDR sources. Well chamber (Plate 3.15) type provides an easy and reliable method for calibrating brachytherapy sources. For the purpose of this research, the HDR 1000 Plus well chamber of reference number 90008 and serial number A083262 from Standard Imaging Inc was used. This chamber was calibrated on November 25, 2008 at Standard Imaging Inc in combination with the electrometer, with the calibration traceable to the United States National Institution of Standards and Technology (NIST) with a calibration co-efficient of $4.824E+05 \text{Gym}^2/\text{h}/\text{A}$. It was designed, manufactured and distributed with a quality management system certified to ISO 9001:2008 and ISO 13485:2003, by Intertek-SEMKO. The chamber has been calibrated to the correlated conditions of the Co-60 high dose rate brachytherapy afterloading source manufactured

by Eckert and Ziegler Bebig GmbH, with temperature and pressure corrected to 22°C and 760mm Hg.

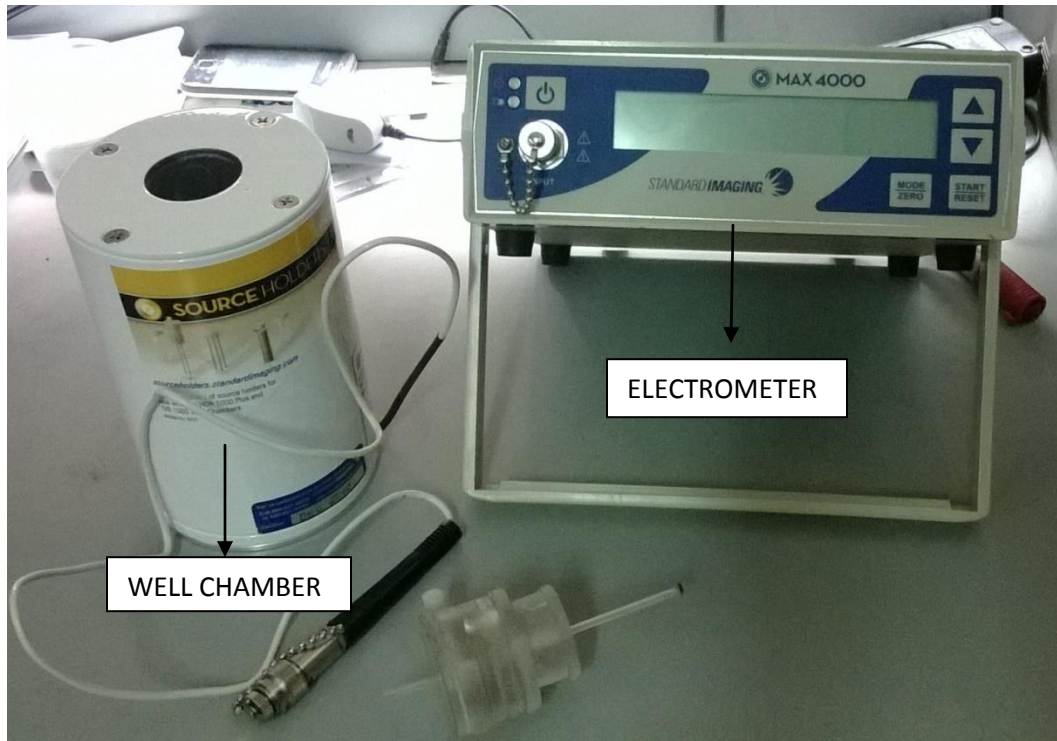


Plate 3.15: The electrometer and well chamber used.

3.2.2 Dose verification tests

3.2.2.1 Determination of calibration point of the well chamber.

The calibration point of a well type chamber is defined as the point at which the centre of the source is positioned during the calibration procedure; this point may differ from one source to another depending on the source length. Some chambers have a fixed, non-removable, spacer in the well and the source is then conveniently placed on the top of the spacer. Other models, on the other hand, have a mechanism to move and fix the source

holder to different heights and the source is then placed at the bottom of the movable holder during the calibration procedures.

In this test, the source holder (Plate 3.16) was designed and constructed from perspex to hold the sources in different positions within the chamber.

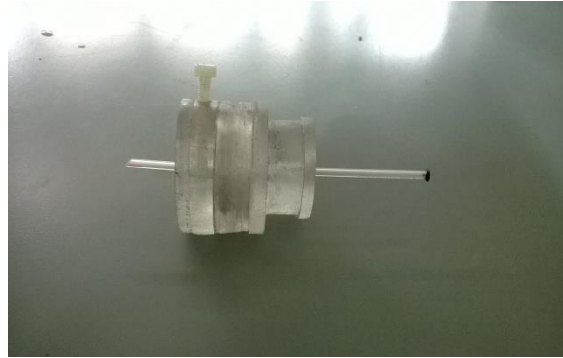


Plate 3.16: The source holder.

The procedure for this test started from the bottom of the chamber, the source holder with a source was retracted in distances of 0.5cm and corresponding current reading in mA from the electrometer was recorded. A calibration curve was plotted (distance against current) using microsoft excel (Graph 4.1). The maximum point was located, therefore became the calibration point and was used for this work.

3.2.2.2 Verification of source strength.

It is recommended that after the receipt of a batch of seed sources, a random sample containing 10% of the seeds should be verified in terms of source strength with the source strength produced by the manufacturer and should fall within $\pm 3\%$ of the manufacturer's value (Kutcher et al, 1994).

In this test, the electrometer was first turned on with nothing connected to the input jack of the electrometer and waited for about 10 minutes for warm up then the leakage of the electrometer was verified. Subsequently the well chamber was connected to the electrometer and a +300 V bias voltage was applied. The electrometer and the well chamber system were allowed at least 10 minutes to stabilize. The leakage was measured again by measuring charges without the I -125 seed source in the chamber. Then, the electrometer was zeroed by activating the zeroing knob on the console of the electrometer. Again the system leakage was determined and was found to be less than 0.1% of the final signal expected. With the aid of a barometer and a thermometer the atmospheric pressure and temperature were measured. The radiation source was then inserted into the source holder and placed into the well chamber. Three readings from the electrometer were recorded. The data were analyzed by taking into account the average of the readings, system leakage, temperature / pressure corrections and calibration factors by using the equations 3.1 and 3.2. Results are shown in Table 4.7.

$$S_K = M_{raw} \times C_{TP} \times C_A \times C_{LDR} \times N_{SK} \quad (3.1)$$

$$M_{corr} = M_{raw} \times C_{TP} \times C_A \times C_{LDR} \quad (3.2)$$

$$C_{TP} = \frac{273.15 \times T(^{\circ}C)}{295.15} \times \frac{760}{P(Torr)} \quad (3.3)$$

$$C_A = K_1 \times [P(Torr)]^{K_2} \quad (3.4)$$

Where:

S_K = The air kerma strength of the source in U. 1U= $\mu\text{Gym}^2/\text{h}$

M_{raw} = The reading in mA.

C_{TP} = The temperature and pressure correction factor.

C_A = The calibration factor for the electrometer scale.

N_{SK} = The HDR 1000 plus calibration co-efficient.

C_{LDR} = the conversion factor from HDR to LDR

3.2.2.3 Treatment planning dose verification

Fourteen $2 \times 3 \text{ cm}^2$ cut films were calibrated in a 1.25MeV photon beam produced by a Theratron Equinox 100 Co-60 Teletherapy unit in the dose range of 0, 25, 50, 75, 100, 125, 150, 175, 200, 225, 250, 275, 300, and 325 cGy. The exposed film samples were analyzed not right after irradiation in order to ensure optimum growth of optical density. The films were digitized in the reflective mode using an Epson scanner (Epson stylus CX5900). Images were acquired in "professional mode" with the image type set to 24-bit RGB, resolution 72 dpi and the data were saved as JPEG.

With the help of the ImageJ software, the mean pixel value was then obtained for each calibration film. A dose response curve for the Gafchromic EBT2 film was plotted between the mean pixel density and corresponding value of the dose and a fit equation was generated. (Figure 4.2)

Forty- five I-125 seed sources were inserted into the perspex prostate phantom because in general, patients undergoing prostate brachytherapy can be implanted with seeds ranging from 45- 90 (Khan, 2005). For the purpose of this work, film samples of size $14 \times 2 \text{ cm}^2$ with six calculation points were positioned in-between the loaded perspex slabs. The films were replaced after every 24 hours for 10 days and scanned after the 10th day.

The exposed films were digitized in an identical way during the calibration, and their images were acquired. The images were digitized and their pixel values along the

longitudinal and transverse bisectors of the film were obtained. Image J was used to compute the mean pixel value of the irradiated films. This was done in the red colour channel, the film manufacturer recommended using the red channel component of the image normalized to the blue channel component in order to eliminate the effect of film thickness variations. However, despite the fact that errors due to the thickness of the active layer were correlated for the red and blue channels, it was found that other components, such as the intrinsic noise from the scanner readings, nevertheless increased the overall uncertainty. It was found that using only the red component was a better choice over using the red and blue correction, as suggested in the ISP white paper (Wayne, 2009). The mean pixel value found in each case was converted into doses applying the obtained fit equation (Eq 4.1). With the help of Microsoft excel, the doses were accurately computed and deviations measured.

A computed tomography (CT) scan of slice thickness 0.3cm was taken for the perspex prostate phantom loaded with the I- 125 seeds and images imported unto the treatment planning system (TPS), planned accordingly and evaluated. Doses at each calculation point were determined and compared to that of the Gafchromic film. The relative error was deduced by subtracting the doses obtained from the Gafchromic film from that obtained from the TPS.

CHAPTER FOUR

RESULTS AND DISCUSSION

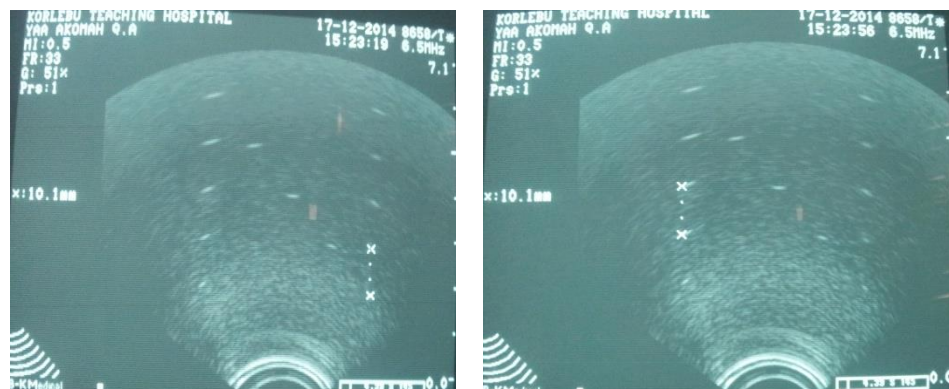
In this chapter, the analysis of the results obtained and discussions are presented. The results are grouped into performance evaluation and dosimetry.

4.1 Performance evaluation results

Seven tests were performed on the ultrasound brachytherapy system to assess its functionality and suitability for accurate treatment planning and dosimetry. Results for axial distance measurement accuracy, lateral distance measurement accuracy, volume measurement accuracy, depth of penetration, and axial and lateral resolution tests, physical grid alignment and internal grid alignment and probe retraction accuracy are presented in Appendix A and a summary presented in Table 4.1 - Table 4.6 respectively.

4.1.1 Axial distance measurement accuracy

With the help of the electronic calipers on the ultrasound scanner, axial distances between targets along columns B and F (Plate 4.1a,b) were measured on the ultrasound image and compared with the standard inter-targets distances of 10 mm produced by the manufacturer of the phantom. For column B, the average inter-target distances between B1-B2, B2-B3, B3-B4 and B4-B5 were 10.12 ± 0.08 mm, 10.12 ± 0.12 mm, 10.11 ± 0.10 mm and 10.12 ± 0.10 mm respectively.



a)

b)

Plate 4.1a,b: Axial measurements on Columns B and F respectively.

The estimated overall average inter-target distance for column B was $10.12 \pm 0.1\text{mm}$ amounting to approximately 1.2% increase in the standard inter-target distance of 10 mm. Also, along the F column, the average inter-target distances between F1-F2, F2-F3, F3-F4 and F4-F5 were $10.09 \pm 0.10\text{ mm}$, $10.11 \pm 0.09\text{ mm}$, $10.11 \pm 0.07\text{ mm}$ and $10.10 \pm 0.19\text{ mm}$ respectively and the overall average inter-target distance was estimated to be $10.10 \pm 0.11\text{ mm}$, deviating by approximately 1.0% from the 10 mm standard inter-target distance (see Table 4.1).

With tolerance levels of $\pm 2\text{ mm}$, $\pm 1\%$, $\pm 1.5\%$, $\pm 1\%$, $\pm 2\%$, $\pm 1\text{ mm}$ and $\pm 2\%$ error margin recommended by AAPM TG 128 (Pfeiffer et al, 2008), NCRP report number 99 (NCRP , 1999), Grammex/RMI, AAPM TG 1 (Goodsitt et al, 1998), AIUM (1990), CAPCA and AAPM 43rd annual meeting (Kofler, 2001) respectively, it was deduced from the results that the ultrasound system produces a good level of accuracy in axial measurements. These results indicate that for patient studies, the system can be relied

upon to measure accurate axial distances between different brachytherapy seeds or between seeds and the rectal wall.

Table 4.1: Axial distance measurement accuracy results.

	B1-B2	B2-B3	B3-B4	B4-B5	F1-F2	F2-F3	F3-F4	F4-F5
Expected distance (mm)	10.00	10.00	10.00	10.00	10.00	10.00	10.00	10.00
Measured average distance (mm)	10.12±0.08	10.12±0.12	10.11±0.10	10.12±0.10	10.09±0.10	10.10±0.09	10.11±0.07	10.10±0.19
Abs. difference	0.12	0.12	0.11	0.12	0.09	0.10	0.11	0.10
difference (%)	1.20	1.20	1.10	1.20	0.90	1.00	1.10	1.00

4.1.2 Lateral distance measurement accuracy

Lateral distances measured between targets along the rows 1, 2, 3 and 4 on the ultrasound image (Figure 4..2) are presented in Table 4.2. Measured distances were compared with known inter-target distances of 10 mm for B4–C4, 20 mm for B3–D3, 30 mm B2–E2, and 40mm for B1–F1 (Plate 4.2).

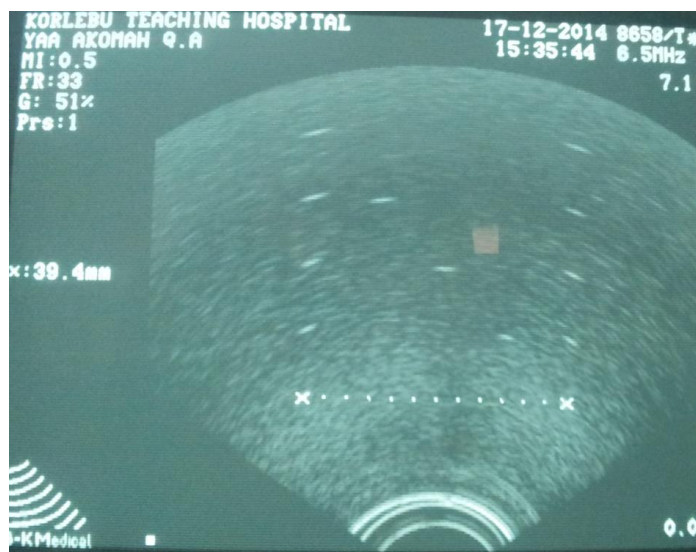


Plate 4.2: Lateral distance measurement along B1-F1

Estimated average distance for B4–C4 was 10.07 ± 0.06 mm, deviating from the standard inter-target distance of 10 mm by approximately 0.07 mm or ± 0.7 %. Average distance for B3–D3 was 20.01 ± 0.07 , deviating from the 20 mm standard inter-target distance by 0.01 mm or ± 0.05 %. For targets B2–E2, the average distance was 29.56 ± 0.33 mm, deviating from 30 mm standard inter target distance by approximately -0.44 mm or -1.47 %. Also for targets B1-F1, the average distance was 39.54 ± 0.38 mm, deviating from the standard inter-target distance of 40 mm by approximately -0.46 mm or -1.15 %.

Deviations in all four sets of measurements fell within the tolerance levels ± 3 mm, ± 3 %, ± 2 %, ± 2 %, ± 2.5 % and ± 3 % recommended by AAPM TG 128 (Pfeiffer et al, 2008), AIUM (1995), , Grammex/RMI (1994), AAPM TG 1 (Goodsitt et al, 1998), NCRP report number 99 (NCRP , 1990) and AAPM 43rd annual meeting (Kofler, 2001) respectively. This indicates a good level of accuracy in the measurement of lateral distances

within the prostate organ during brachytherapy procedures. Tolerance level for lateral distance accuracy is always greater than axial accuracy due to reduced spatial resolution in the lateral direction, leading to increased uncertainty in the position of the target.

Table 4.2: Lateral distance accuracy measurements results

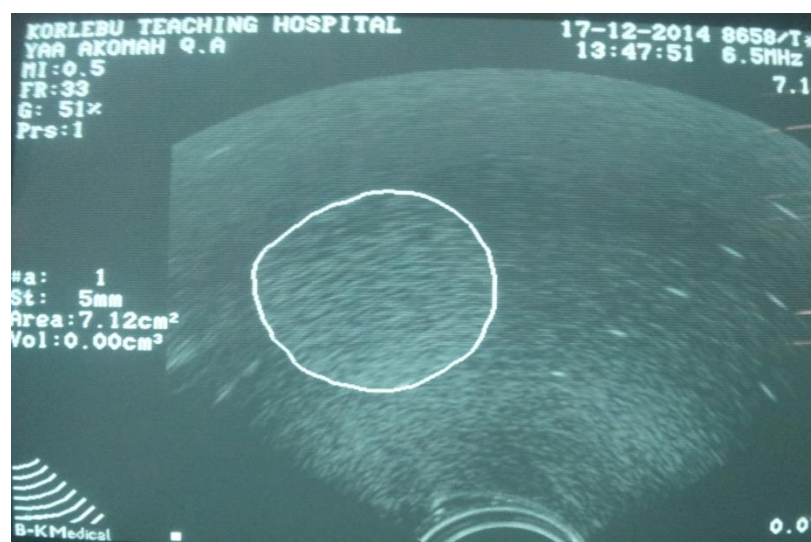
	B4-C4	B3-D3	B2-E2	B1-F1
Expected distance (mm)	10.00	20.00	30.00	40.00
Measured average distance(mm)	10.07±0.06	20.01±0.07	29.56±0.33	39.54±0.38
Absolute difference	0.07	0.01	0.44	0.46
Percentage difference (%)	0.7	0.05	-1.46	-1.15

4.1.3 Volume measurement accuracy

The ability of an ultrasound brachytherapy system to accurately determine the volume of a target (Plate 4.3) is very important for real time dosimetry. Results for the three dimensional standard target volumes measured during the course of this study are presented in Table 4.3. The measurements of the volumes 4 cm³, 9 cm³ and 20 cm³ produced average measurements of 3.97±0.16 cm³, 8.86±0.29 cm³ and 20.11±1.04 cm³, resulting in approximate deviations of -0.75 %, -1.56 % and 0.55 % respectively. Percentage deviations of all three target volumes were within the tolerance of ±5 % specified by AAPM TG 128 (Pfeiffer et al, 2008) and CAPCA.

Table 4.3: Results of volume accuracy measurements

	Volume 1	Volume 2	Volume 3
Expected measurements (cm ³)	4.00	9.00	20.00
Average measured volume (cm ³)	3.97±0.16	8.86±0.29	20.11±1.04
Absolute difference	0.03	0.14	0.11
Percentage difference (%)	-0.75	-0.56	0.55

**Plate 4.3: Measurement of volume targets.**

4.1.4 Depth of penetration (DOP)

This test determines how deep into a patient a low contrast object can be visualized. Results for the depth of penetration or sensitivity are presented in Table 4.4. The average depth of penetration was estimated to be 5.37 ± 0.04 cm, implying that a low contrast object or organ can be visualized approximately 5.4 cm into a patient on the ultrasound system. Depth of penetration can be affected by change in signal to noise ratio (SNR).

Decrease in SNR causes a decrease in maximum depth of penetration clinically. When this occurs, the anterior boundary of an imaged prostate gland becomes difficult to visualize. At the time of performing this test, there was no available depth of penetration for the ultrasound system, hence comparison with measured depths was not possible.

Table 4.4: Results of depth of penetration.

	Depth of penetration		
	Test 1	Test 2	Test 3
Average measured depths(cm)	5.39±0.06	5.35±0.04	5.36±0.03

4.1.5 Axial and lateral resolution accuracy

The axial and lateral resolution tests were performed with the probe in the axial and longitudinal arrays. Results for this test are presented in Table 4.5. Measurements in the axial array resulted in an average axial and lateral resolutions of 0.60 ± 0.07 mm and 1.89 ± 1.20 mm respectively. It was noticed that in this array, lateral resolution measured in columns B and F showed increase in target size in the image as the probe moves from row 1 to row 2. Also in the longitudinal array, an average axial resolution of 0.33 ± 0.13 mm was estimated while an average resolution of 1.76 ± 0.26 mm was estimated in the lateral direction. It was also noticed that the average lateral resolution in the longitudinal array showed increase in target size on the image as compared with the axial resolution in

the same array. Tolerance level for this test could not be assessed due to the unavailability of manufacturer's data to compare measured results with.

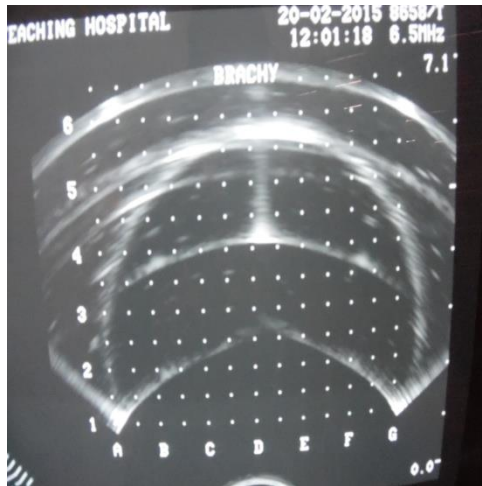
Table 4.5: Results on axial and lateral resolution

	Axial array		Longitudinal array	
	Axial resolution	Lateral resolution	Axial resolution	Lateral resolution
Ave. measured resolution (mm)	0.60±0.07	1.89±1.20	0.33±0.13	1.76±0.26

4.1.6 Physical grid alignment accuracy/ internal grid alignment accuracy.

This test also determines how needles can be physically inserted according to the pre-plan. After inserting needles into 6A, 6G, 1A, 1G and 4D positions on the physical template (Plate 4.4b), needle deviations from these positions on the image (Plate 4.4a) obtained were recorded and the maximum discrepancy was presented in Table 4.7. Positions 1A and 1B did not show any discrepancy, it was well aligned, but positions 6A, 6G and 4D showed some discrepancies. At position 4D the discrepancies were 2.05±0.02 mm and 1.45±0.01 mm to the right and top respectively, at position 6A discrepancies were 2.67±0.01 mm and 1.05±0.01 mm to the right and top respectively and position 6G showed discrepancies of 1.85±0.02 mm and 1.64±0.01 mm to the right and top respectively. The maximum discrepancy occurred at position 6A. The maximum discrepancy, 2.67±0.01 mm measured was within the tolerance level of 3.00 mm

provided by AAPM TG 128 (Pfeiffer et al, 2008). Some discrepancy may be observed due to beveled needle tip that may deflect from the path initiated by the physical template. This may account for discrepancies seen between on-screen template correspondence in water and in tissue. From the results obtained in this study, the template and electronic/internal grid are well aligned physically and internally, therefore needles can be accurately inserted according to the preplan requiring no intraoperative corrections.



a)



b)

Plate 4.4a,b: Ultrasound image of needles and set-up for grid alignment accuracy respectively.

Table 4.6: Results of physical template alignment accuracy measurements.

	Needle positions on template					
	4D		6A		6G	
	Right	Top	Right	Top	Right	Top
Average	2.02±0.02	1.45±0.01	2.67±0.01	1.05±0.01	1.85±0.02	1.64±0.01
measured discrepancy(mm)						

4.1.7 Probe retraction accuracy.

The purpose of this test was to test the stepping mechanism for accurate seed placement in the z-axis. From the crossing wire number 6, with two clicks (1.0 cm) on the stepping device the next crossing wire (number 5) was seen in the same way also with two clicks the next crossing wire was seen (number 4), the next crossing wire (number 3) was also seen in two clicks. The next crossing wire (number 2) was seen in the next click (0.5 cm) and the last crossing wire (number 1) was seen in the next click. The results indicate that the stepper or stepping mechanism is performing well therefore seeds are accurately being placed in the z-axis.

4.2 TPS dose verification results

The results for the dosimetry tests of the seed implants are presented in Appendix B. The results discussed are the calibration point tests, the source strength verification tests, and

the treatment planning dose verification tests. The summary of the results are presented in Figure 4.1, Figure 4.2, Figure 4.3, Table 4.7 and Table 4.8.

4.2.1 Calibration point test.

The calibration point of a well type chamber is defined as the point at which the centre of the source is positioned during the calibration procedure. The calibration point is the most sensitive position in the chamber where measurement for a particular type of seed implant is done. Therefore, the purpose of this test was to identify the position in the chamber that recorded the maximum amount of current (mA). The results for calibration test point are presented in Figure 4.1. The graph indicated the maximum current at 3 cm. For the purpose of this study, all measurements were taken at this point.

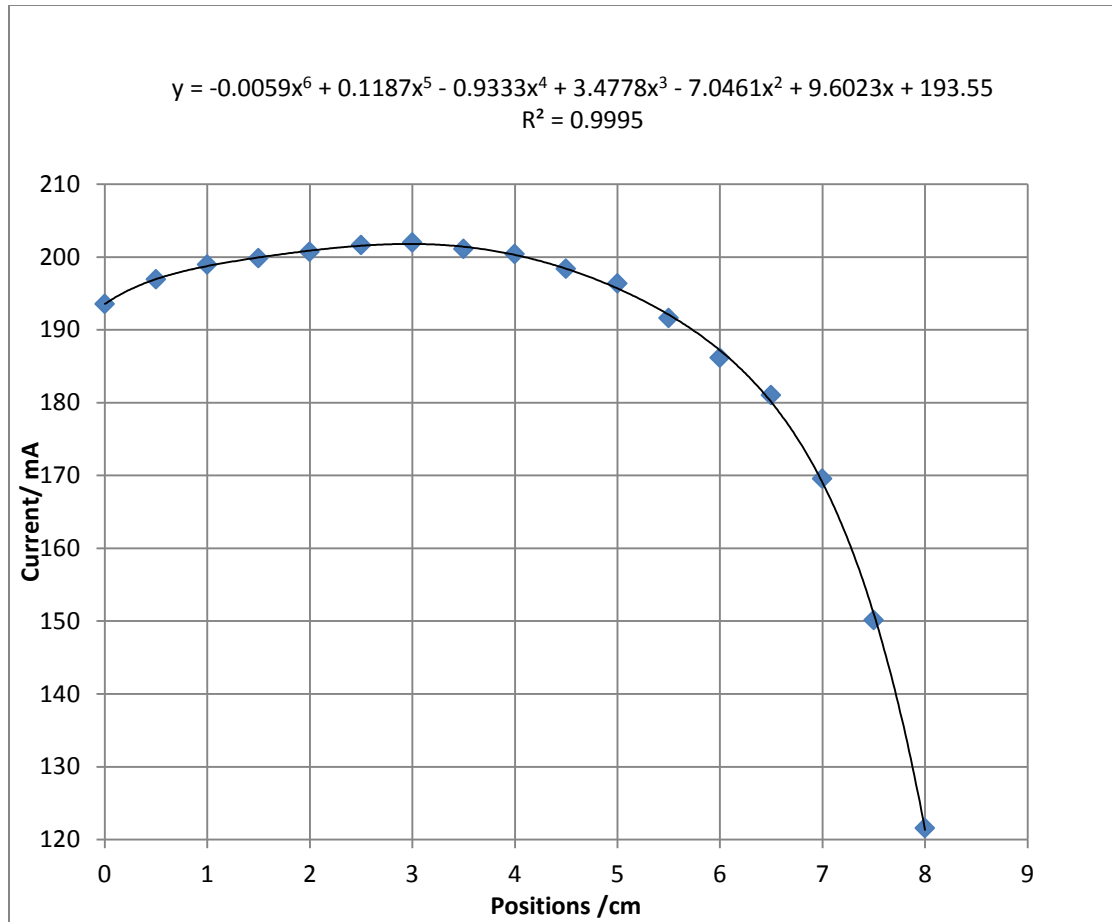


Figure 4.1: A graph of current (mA) against positions (cm).

4.2.2 Source strength verification test.

Before clinical use of a brachytherapy source, regulations or recommendations by medical physics societies require an independent measurement of its reference air kerma strength by a qualified medical physicist. Results for this test are presented in Table 4.7. It is measured in unit of U i.e. $1U = \mu\text{Gym}^2/\text{h}$ as defined by ICRU report 38 (ICRU, 1985). It was observed that the average source strength measured was $0.651450 U \pm 0.001052 U$. This value takes account of decay correction and was compared to a decay

corrected manufacturer's value of 0.64989 U resulting in a percentage difference of 0.242 % \pm 0.164 % which is within the accepted tolerance value of ± 3 % (Nath et al, 1997).

Therefore the seed sources used in this work have passed the test.

Table 4.7: Source strength verification results.

	Source strength
Average measured strength (U)	0.651458 \pm 0.001052
Expected measurements (U)	0.64989
Absolute difference	0.001570 \pm 0.001052
Percentage difference (%)	-0.242 \pm 0.164

4.2.3 Treatment planning dose verification test.

The first step in this test was to generate the best fit equation from the dose response curve of the calibrated Gafchromic EBT2 films. The dose response curve between the mean gray value and dose obtained for the calibrated Gafchromic EBT2 film is presented in figure 4.2. It was observed that as the mean gray value decreases the dose increases exponentially. The dose read from the calibrated films yielded errors between 0 to 7.6%, which is above the action limit of 5% (Appendix B). This may have occurred due to mishandling of the film and also the unavailability of the appropriate illumination for film storage. The best fit equation (4.1) generated from the dose response curve was used to generate the doses after the mean pixel values have been obtained from the films (14 x 2 cm²). The variation in the film intensity is related by an exponential function.

$$y = 1.776.9 \times e^{-0.044x}$$

4.1

Where, x is the mean gray value, and y is the dose. The dose at each calculation point was determined, summed and multiplied by a factor of 9.4 to account for the total dose at the 94th day from the implant day of the seed (day of planning). The calculation points were six in all meanwhile; the calculation points 1 and 5 yielded the highest doses amongst the others due to their locations in the phantom (Figure 4.4). Results for this test are presented in Table 4.8. Figure 4.3 is a graph that shows the variation of the measured dose from the Gafchromic films and those from the TPS.

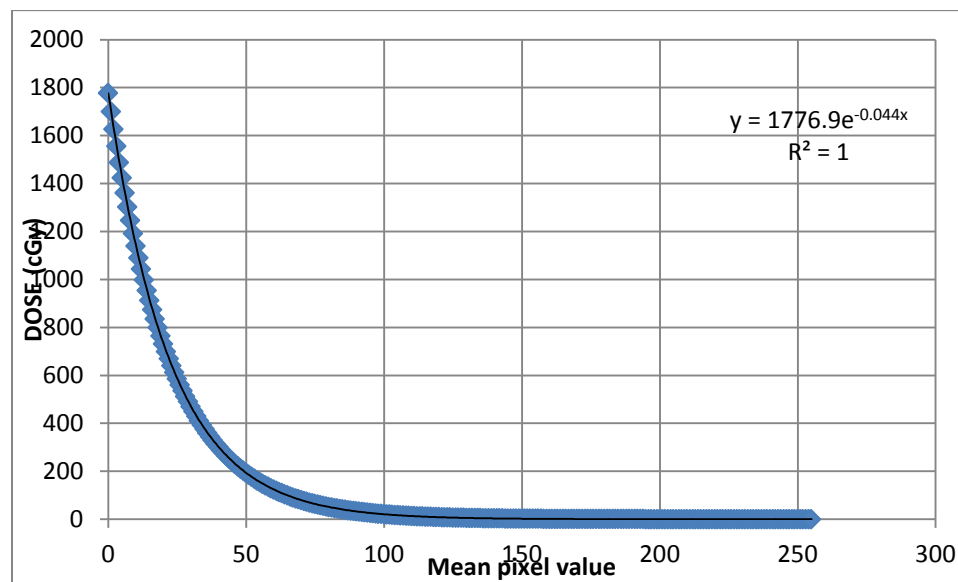


Figure 4.2: The dose response curve for the calibrated Gafchromic EBT2 film.

Table 4.8: Results for the TPS dose verification test

	Dose (cGy)					
	Calc. Pt. 1	Calc. Pt. 2	Calc. Pt. 3	Calc. Pt. 4	Calc. Pt. 5	Calc. Pt. 6
Relative error	0.228381	0.246584	0.184026	0.270573	0.068908	-0.12645
Error (%)	22.838100	24.658400	18.402600	27.057300	6.890800	-12.64500

The percentage errors obtained in Table 4.8 are significant, this may have occurred due to postirradiation development of the films with time. In order to reproduce the same scanning parameters for all ten films, all ten were scanned the same day causing the extension of postirradiation development which should have been 48hours postirradiation. During this extended period of postirradiation, temperature and relative humidity may have influenced postirradiation colouration. Also, the errors that could have occurred during calibration may have attributed to this significant error. This new development was realized after all ten films were scanned but due to the unavailability of new and fresh implant seeds, the process could not be repeated. However, the same pattern was realized for both the TPS and Gafchromic doses. As shown in Figure 4.4, the calculation points X1 and X5 on the Gafchromic films received the most seed contributions due to their positions in the phantom while calculation points X4 and X6 had the least seed contributions as compared to the other calculation points. After reading the films, the doses followed the pattern of seeds contributions according to their seed arrangements within the phantom (Figure 4.4). In the same way also the doses produced by the TPS followed the same trend.

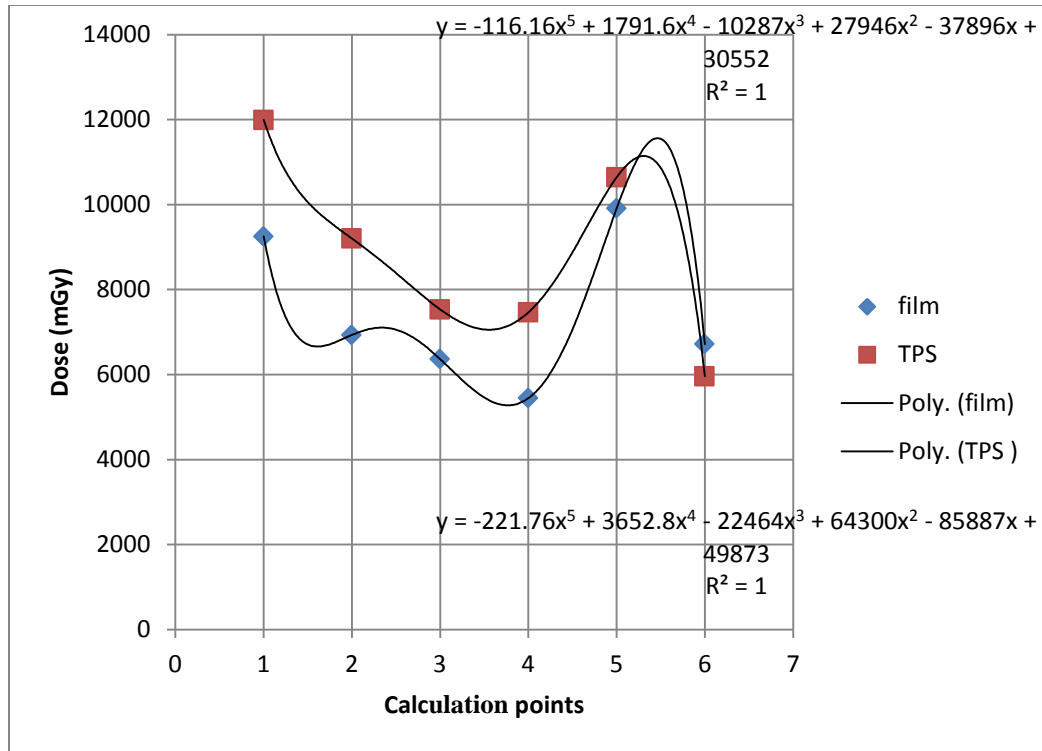


Figure 4.3: A graph showing the differences in TPS and measured dose.

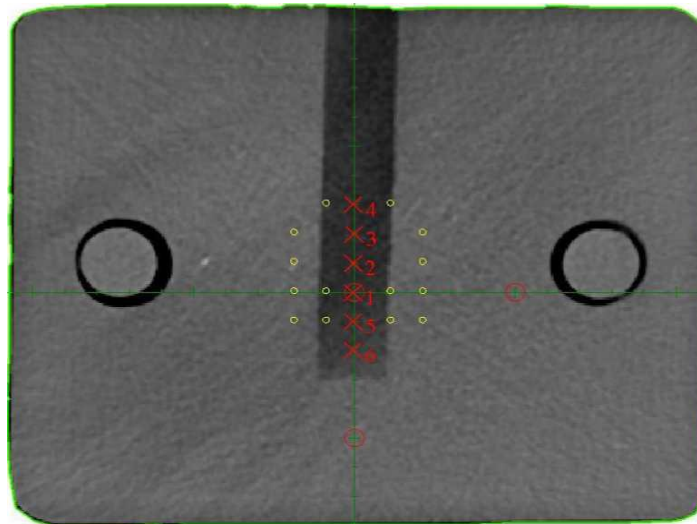


Plate 4.5: A CT slice of the perspex prostate phantom showing the calculation points.

4.3 Limitation

The challenges encountered during this work include:

- Non-availability of a LDR source holder calibrated for ^{125}I sources
- The ^{125}I sources used had reached their half life and
- The failure of the Gafchromic film in a water phantom. The later occurred as a result of the penetration rate to the Gafchromic film in water. Results from Martin, Chang and Peter in 2000, show that within 24 hours the visible penetration is less than 5mm at the edges of the film. Meanwhile the width of the film used was 0.8cm.

Table 4.9: Recommended tolerances and findings.

QC TEST	CAPCA (2007)	AIUM (1995)	GRAMMEX (1994)	GOODSITT ET AL(1998)	NCRP (1990)	KOFLER (2001)	PFEIFFER ET AL (2008)	FINDINGS FROM WORK
Depth of penetration	-	±1cm	±1cm	±1cm	±1cm	±1cm	±1cm	±0.06cm
Axial Resolution	-	0	-	1mm	-	N/A	±1mm	±0.13mm
Lateral resolution	-	0	-	1mm	-	±0.5mm	±1mm	±1.20mm
Axial distance	1mm	±2%	±1%	±1.5%	±1%	±2%	2mm or 2%	±0.11mm
Lateral distance	1mm	±3%	±2%	±2%	±3%	±2.5%	3mm or 3%	±0.46mm
Volume measurement	3%	-	-	-	-	-	5%	0.55%
Needle template alignment	1mm	-	-	-	-	-	3mm	2.67mm
Probe retraction	1mm	-	-	-	-	-	0	0

CHAPTER FIVE

CONCLUSION AND RECOMMENDATION

This chapter presents conclusions from this research study on the performance evaluation of the ultrasound system and prostate brachytherapy system and TPS dose verification and associated recommendations.

5.1 Conclusion

The purpose of this study was to provide baseline measurements for the first time in Ghana for the prostate brachytherapy system characteristics and to enhance the treatment of the prostate cancer. In achieving the objective of this study, several tests were conducted on the ultrasound system and prostate brachytherapy system. The treatment planning system dose verification was also done. Performance evaluation tests on the ultrasound brachytherapy system included axial distance measurement, lateral distance measurement, volume measurement, depth of penetration, physical / internal template grid alignment, probe retraction test and axial and lateral resolution. Except for depth of penetration and resolution tests in which baseline data were not available for comparison, all other quality control tests on the ultrasound system fell within set tolerances as recommended by the American Association of Physicists in Medicine Task Group Report 128 (Pfeiffer et al, 2008), AIUM (1995), Grammex/RMI (1994), AAPM TG 1 (Goodsitt et al, 1998), NCRP report number 99 (NCRP , 1999) and AAPM 43rd annual meeting (Kofler, 2001). Table 4.9 provides a summary of recommended tolerances used

in the work as well as findings from the work. It can be concluded that the permanent LDR brachytherapy system is performing well.

For dose verification, the measurements conducted were: the calibration point test, source strength verification and the TPS dose verification. The calibration point test indicated that the distance for maximum ionization chamber sensitivity is 3cm, so seeds can be calibrated at this point. The source strength verification was within the tolerances recommended by ICRU report 38 (ICRU, 1985). The TPS dose verification test produced results with significant errors which occurred due to postirradiation development of film with time, the use of seeds that were already decayed passed its half life and also errors that occurred in the calibration film dosimetry but both doses generated by the TPS and Gafchromic film followed the same pattern. The outcome of the performance evaluations indicate that for patient work, the ultrasound system and prostate brachytherapy system can provide the mechanism for accurate positioning of the brachytherapy seeds facilitating reliable identification of the target volume for effective treatment.

5.2 Recommendation

The following are the Recommendations made to the various stakeholders at the National Centre for Radiotherapy and Nuclear Medicine at the Korle-Bu Teaching Hospital (KBTH).

5.2.1 National Centre for Radiotherapy and Nuclear Medicine

It is recommended that the Management of the Centre should establish a QC committee with the following functions:

- Establish a QA/QC program for periodic evaluation of the performance of the prostate brachytherapy system and verification of treatment planning and dosimetry accuracy using the findings of this study as baseline information for quality improvement.
- Establish a QC plan consistent with recommendations in Appendix C of this thesis.
- Establish a mechanism for monitoring and evaluation of the effectiveness of the treatment with prostate brachytherapy system and its associated Treatment planning system.
- Purchase accompanying QC kits and phantoms when acquiring new equipments.
- Performance evaluation tests should be done for the new system at KBTH.

5.2.2 Regulatory Authority

- Provide a regulatory guidance performance standards, safe and effective use of the prostate brachytherapy system and its associated Treatment Planning System (TPS).

5.2.3 Future research studies

- It is recommended that the use of another dosimetric system aside the gafchromic film should be used to verify the TPS dose.

REFERENCES

- AIUM Technical standards committee (1995), *Quality control manual for gray – scale ultrasound scanners – stage 2*. American institute of ultrasound in medicine: Laurel MD
- Anderson L. L, Nath R., Olch A. J., and J. Roy (1991), “*American Endocurietherapy Society recommendations for dose specification in brachytherapy*,” *Endocuri./Hyperther. Oncol.* 7, 1-12.
- Aronowitz J. N., Rivard M. J. (2013); *The phylogeny of permanent prostate brachytherapy*. 10.5115/jcb. 2013.35562.
- B. R. Prestidge, W. S. Bice, E. J. Kiefer, and J. J. Prete (1998), “*Timing of computed tomography-based postimplant assessment following permanent transperineal prostate brachytherapy*,” *Int. J. Radiat. Oncol., Biol., Phys.*40, 1111–1115.
- Badiozamani K. R., Mate T. P. and Gottesman J. E. (2005); *High dose rate Ir-192 prostate brachytherapy*. Basic and advanced techniques in prostate brachytherapy. Chapter 3, pg 295, 2005, ISBN 1841842982
- Beyer, D., Nath, R., Butler, W., Merrick, G., Blasko, J., Nag, S. and Orton, C. (2000), “*American Brachytherapy Society recommendations for clinical implementation of NIST-1999 standards for 103 Palladium brachytherapy*”. *Int. J. Radiat. Oncol. Biol. Phys.* 47, 273-275.
- Bice, W., Preslidge, B., Prete, J. and Dubois, D.(1998), “*Clinical impact of implementing AAPM Task Group 43 on permanent prostate brachytherapy using I-125*”. *Int. J. Radiat. Oncol. Biol.Phys.* 40, 1237-1241.
- Bilaniuk N. and Wong G. S. K. (1996), “Speed of sound in pure water as a function of temperature” *J J. Acoust. Soc. Am.* 93(3), 1609-1612, as amended by Bilaniuk N. and Wong G. S. K (1993), Bilaniuk N. and Wong G. S. K. , “speed of sound in pure water as a function of temperature” *J. Accoust. Soc. Am.* 93, 1609-1612, *J. Accoust. Soc. Am.* 99. 3257.
- Board of the faculty of clinical oncology, the Royal College of Radiologist, *Quality assurance practice guidelines for transperineal LDR permanent seed brachytherapy of prostate cancer*.
- Brachytherapy cancer index, www.cancerindex.org, July 07,2014, Pg 1.
- Burger W, Burge M. (2007); *Digital Image Processing: An Algorithmic Approach Using Java*. Springer, 2007
- Butson M. J., Cheung T. and Yu P. K. N (2000), *Radiochromic film dosimetry in water phantoms*, *Phys. Med. Biol.* 46 N27 – N31

CAPCA (Canadian Association of Provincial Cancer Agencies) (2007); *Standard for Quality Control at Canadian Radiation Treatment Centres; Low dose rate prostate brachytherapy*.

Charles P. Davis, MD (2014); Prostate cancer facts, MedicineNet.com, Retrieved on 10/26/2014, <http://www.medicinenet.com>.

Chiu-Tsao S.T. and Anderson L.L. (1991); *Thermo luminescent dosimetry for Pd-103 seeds (model 200) in solid water phantom*, Med. Phys. 18, 449-452.

Colleen Lawton, MD, Michael Cillian, PhD, Leonard Gomella, MD, David Grignon, MD, W. Robert Lee, MD,(1998); Radiation therapy oncology group, RTOG 98-05: *Phase II trial of transrectal ultrasound guided permanent radioactive implantation of the prostate for definitive management of localized Adenocarcinoma of the prostate*. Pg. 6

Collins TJ (July 2007), "*ImageJ for microscopy*". BioTechniques 43:S25-S30, Supplement to Volume 43, No. 1.

Dean Wilkinson (2010); *Commissioning of an in vivo dosimetry system for high dose rate gynaecological brachytherapy*, Master of Science thesis, University of Wollongong, Department of Engineering Physics, University of Wollongong, 2010. <http://ro.uow.edu.au/thesis/3277>

Dougherty, G (2009); *Digital Image Processing for Medical Applications*. Cambridge University Press

Douglas Pfeifer, Steven Sutlief, Wenzheng Feng, Heather M. Pierce, Jim Kofler, (December 2008); AAPM Task Group 128: *Quality assurance tests for prostate brachytherapy ultrasound system*. Medical Physics, vol. 35, No. 12, December 2008.

Eliceiri K, Rueden C. (2005), "*Tools for visualizing multidimensional images from living specimens*". Photochemistry and Photobiology. Volume 81, Issue 5.

F. M. Waterman, N. Yue, B. W. Corn and A. Dicker, (1998), "*Edema associated with I-125 or Pd-103 prostate brachytherapy and its impact on postimplant dosimetry: An analysis based on serial CT acquisition,*" Int. J. Radiat. Oncol., Biol., Phys.41, 1069–1077.

F. M. Waterman, N. Yue, S. Reisinger, A. Dicker, and B. W. Corn (1997), "*Effect of edema on the post-implant dosimetry of an I-125 prostate implant: A case study,*" Int. J. Radiat. Oncol., Biol., Phys. 38, 335–339 Faiz M. Khan, The physics of radiation therapy, 3rd Edition, pg 481, 2003, ISBN 978-0-7817-8856-4.

Fuks Z, Leibel S.A, Wallner K.E, Begg C.B, Fair W.R, Anderson LL et al (1991); *The effect of local control on metastatic carcinoma of the prostate: long term results in patients treated with I-125*. Int J Radiat Oncol Biol Phys 21: 537-547.

Gerald K. J., Coia L., Michael G. et al; *Comprehensive QA for radiation oncology, AAPM report no. 46*. Med. Phys. 21 (4) 0094-2405, April 1994.

Girish V, Vijayalakshmi A (2004), "Affordable image analysis using National Institute of Health. Image/ImageJ". Indian Journal for Cancer volume 41, Number 1, page 47.

Godden T.J (1988), *Physical aspects of brachytherapy*, Adam Hilger, Philadelphia.

Goetsch, S.J., Attix, F.H., Pearson, D.W. and Thomadsen B.R. (1991); *Calibration of Ir-192 High dose rate afterloading systems*, Med. Phys. 18, 462-467.

Goodsitt M.M. and Carson P.L., Witt S., Hykes D. L., Kofler Jr J. M., (August 1998); *Report of AAPM ultrasound Task Group No. 1*, Med. Phys. 28 (8),1385-1406 August 1998.

Goodsitt M.M. and Carson P.L., Witt S., Hykes D. L., Kofler Jr J. M., (1998), *Real – time quality control tests procedures*, Med. Phys. (25): p. 1385-1406

Grammex/ RMI (1994), *The QC book for ultrasound*, Middleton, WI : Grammex/ RMI

Grimm P., D.O. Haeney C., PhD, Sylvester J., M.D, and Blasto J., M.D.(November 2003); *Seattle Prostate Institute, Prostate seeds implantation for prostate cancer*; PCRI Insights November 2003 vol. 6, no 4, part 2.

Grimm, P. D., Blasko, J. C., Sylvester, J.E., Meier, R.M. and Cavanagh W. (2001), "10 year biochemical (prostate- specific antigen) control of prostate cancer with I-125 brachytherapy." Int. J. Radiat Oncol Biol Phys 51, 31-40.

Haybittle, J. L. and Mitchell, J. S. (1975), "A simple afterloading technique for the treatment of cancer of the cervix". Br. J. Radiol. 48, 295-298.

Heidenreich A., Bastain, P. J, Bellmunt,J, Bolla,M, Joniau,S, Mason, M.D, Matveev, V, Mottet, N, Van der Kwast, T.H, Wiegel, T, Zattoni, F (2012); *Guidelines on prostate Cancer*, European Association of Urology, IAEA Publication (ISBN 92-0-107304-6).

Henschke, U.K. (1960), "Afterloading" applicator for radiation therapy of carcinoma of the uterus". Radiology 74, 834.

Holm H.H., Juul N., Pedersen F., Hansen H. and Stroyer I. (1983); *Transperineal I-125 seed implantation in prostatic cancer guided by transrectal ultrasonography*. J. Urol. 130,283-286.

Horwitz, H., Kereiakes, J.G., Bahr, G.K., Cluxton, S.E. and Barrett, C.M. (1964); "An afterloading system utilizing Cesium 137 for the treatment of carcinoma of the cervix". Am. J. Roentgenol. Radium Ther. Nucl. Med. 91, 176-191.

IAEA (2004); *Commissioning and quality assurance of computerized planning systems for radiation treatment of cancer*, IAEA Technical Report Series 430, IAEA, Vienna, 2004.

IAEA (June 2006); *Production techniques of quality control of sealed radioactive sources of palladium- 103, iodine- 125, indium -192 and ytterbium-169*. IAEA-TECDOC-1512, June 2006.

ICRU, ICRU report No: 38; *Dose volume specification for reporting intracavitary therapy in gynecology, International commission on radiation units and measurements*, Bethesda, MD.

ISO (2000), International Standard Organization, “*Quality Management Systems, fundamentals and vocabulary*” ISO 9000, 2nd Edition, International organization for standardization, Geneva.

ISP (International Specialty Products) Gafchromic EBT2; *self developing film for radiotherapy dosimetry*, October 7, 2010.

Kofler J. M., Jr. (2001), *Quality assurance of ultrasound imagers : procedures, expectations and philosophies*. AAPM 43RD annual meeting.

Kubo, H., Coursey, B., Hanson, W., Kline, R., Seltzer, S., Shuping, E. and Williamson, J. (1998); “*Report of the Ad Hoc Committee of the AAPM Radiation Therapy Committee on I-125 Sealed Source Dosimetry*”. Int. J. Radiat. Oncol. Biol. Phys. 40, 697-702, 1998(b).

Levin, V.I. et al. (1969); *Separation of 103Pd without a carrier*, Otkrytiya, Izobret, 46(1), 170

Ling, C.C., Li W. X., Anderson L. L., (1995); *The relative biological effectiveness of I-125 and Pd-103*. Int J Radiat Oncol Biol Phys, 32: 373-378.

Ling, C.C., Anderson, L. L. and Shipley, W. U. (1979), *Dose inhomogeneity in interstitial implants using I – 125 seeds*, Inc J Radiat Oncol Biol Phys 5: 419-425.

Ling, C.C., Schell, M. C. and York, E. D. (1985), *Two dimensional dose distribution of I – 125 seeds*, med phys 12, number 5: 652 – 655.

Ling, C.C., York, E. D., Spiro, I. J., Kubiadowicz, D. O. and Bennett, D. (1983), *physical dosimetry of I – 125 seeds of a new design for interstitial implants*, Inc J Radiat Oncol Biol Phys 9: 1747 -1752.

Mayles P., Nahum A., Rosewald C. (2007); *Handbook of radiotherapy physics (theory and practice)*, edition. Pp 1101-1107,1135,36.

N. Suntharalingam, E.B. Podgorsak, H.Tolli (2005); *Radiation Oncology Physics: A Handbook for Teachers and Students*. International Atomic Energy Agency, Vienna 2005. Pages 451-483

Nag, S., Baird, M., Blasko, J. et al. (1997); “*American brachytherapy society (ABS) survey of current clinical practice for permanent brachytherapy of prostate cancer*”. J. Brachyther. Int. 13, 243-251.

Nag, S., Beyer, D., Friedland, J., Grimm, P. and Nath, R. (1999); “*American Brachytherapy Society (ABS) recommendations for transperineal permanent brachytherapy of the prostate*”. Int. J. Radiat. Oncol. Biol. Phys. 44, 789-799.

Nag, S., Bice, W., DeWyngaert, K., Prestidge, B., Stock, R. and Yu, Y. (2000); “*The American Brachytherapy Society recommendations for permanent prostate brachytherapy postimplant dosimetric analysis*”. Int. J. Radiat. Oncol. Biol. Phys. 46, 221-230.

Nath R., Anderson L.L., Meli A. J., Stitt A. J.(1997); Williamson F.J.; *Code of practice for brachytherapy physics: Report of the AAPM Radiation Therapy Committee Task Group No. 56*. Med phys. 24 (10), 1557-1598.

Nath, R., Anderson, L.L., Luxton, G., Weaver, K.E., Williamson, J.F. and Meigooni, A.S. (1995); “*Dosimetry of interstitial brachytherapy sources: Report of the AAPM Radiation Therapy Committee Task Group No. 43*”. Med. Phys. 22, 209-234.

NCS, Netherlands Commission on Radiation Dosimetry. Visser, A.G., Aalbers, A.H.L., Burgers, J.M.V., van der Linden, P.M., Meertens, H., van der Steen, J. and Venselaar, J.L.M. “*Aanbevelingen voor dosimetrie en kwaliteitscontrole van radioactieve bronnen bij brachytherapie*”. Report No. 4 of NCS, Delft, 1989 (in Dutch; with synopsis in English: “*Recommendations for dosimetry and quality control of radioactive sources used in brachytherapy*, NCS 1991).

NCRP, *Quality assurance for diagnostic imaging*, NCRP report No. 99, 1990, National Council for radiation protection, Bethesda.

Pasteau O (1911); *Traitement du cancer de la prostate par le radium*, Rev Mal Nutr 363-7.

Paterson, R. and Parker, H. M. (1934); *A dosage system for gamma ray therapy*, Br. J. Radiol., 7, 592-632.

Paterson, R. and Parker, H. M. (1938); *A dosage system for interstitial radium therapy*, Br. J. Radiol., 11, 313-339.

Redpath, A.T. and Douglas, M.A. (1976); “*The Edinburgh afterloading technique for carcinoma of the uterine cervix*”. Br. J. Radiol. 49, 963-965.

Ridings, G.R. (1963); “*Fractionated intrauterine radium applications: use of a small-diameter afterloading intrauterine applicator. Preliminary report*”. Am. J. Roentgenol. Radium Ther. Nucl. Med. 89, 500-501.

Rivard M. J, Butler W. M, Devlin P. M et al (2007); *American Brachytherapy Society recommends no change for prostate permanent implant dose prescriptions using iodine-125 or palladium-103*. Brachytherapy2007; 6: 34-37.

Rivard M. J., Coursey B. M., Deward L. A., Hanson W. F., Huq M. S., Ibbott G. S., Mitch M. G., Nath R., Williamson J. F. (2004); Update of AAPM TG No. 43 Report:

A revised AAPM protocol for brachytherapy dose calculations. (2004). Med. Phys., 31, 633-674.

Roy J. N., Ling C. C., Wallner K. E., and Anderson L. L. (1996), “*Determining source strength and source distribution for a transperineal prostate implant,*” Endocurietherapy/Hyperthermia Oncol.12, 35–41.

Roy J. N., Wallner K. E., Harrington P. J., Ling C. C., and Anderson L. L. (1993), “*A CT-based evaluation method for permanent implants: Application to prostate,*” Int. J. Radiat. Oncol., Biol., Phys. 26, 163–169.

Seltzer, M., Lamperti, P., Loevinger, R., Soares, C. and Weaver, J. (1998); “*New NIST air-kerma strength standards for I-125 and Pd-103 brachytherapy seeds*”. Med. Phys. 25, A170.

Shalek, R. J. and Stovall, M.(1975); *Use of computers for the calculation of dose from iridium 192 implants, in Afterloading: 20 years of experience 1955-1975*, Hilaris, B. S., Ed., Memorial Sloan-Kettering, New York, pp. 87-89.

Stamey T.A, Yang N, Hay A.R, McNeal J.E, Freiha F.S and Redwine E.(1987); *Prostate- specific antigen as a serum marker for Adenocarcinoma of the prostate.* NEJM 317: 909-916.

Stovall, M., and Shalek, R. J. (1972); *A review of computer techniques for dosimetry of interstitial and intracavitary radiotherapy, Comput. Programs Biomed., 2, 125-136.*

Suit, H.D., Moore, E.B., Fletcher, G.H. and Worsnop, R. (1963); “*Modification of Fletcher ovoid system for afterloading, using standard-sized radium tubes (milligram and microgram)*”. Radiology 81, 126-131.

Tarapcik, P., Mikulaj, V., *Separation of palladium-103 from cyclotron irradiated targets*, Radiochem. Radioanal. Lett., 48 (1981) 1969, 46

Tudway, R.C. (1953); “*The use of radio-active isotopes in applicator for the treatment of carcinoma of the cervix uteri*”. Acta Radiol. 39, 415-422.

Uniyal et al (2012), *Radiochromic film dosimetry of rectal inhomogeneity*, Journal of applied clinical medical physics, Vol. 13 No.1

Varian medical services Inc., 1999-2014

Varian medical systems (July 2006), P/N DOC VS7.2UG.

Wayne, NJ (2009): ISP Corp. *Gafchromic EBT2 self-developing film for radiotherapy dosimetry*. Available from:

http://online1.ispcorp.com/_layouts/Gafchromic/content/products/ebt2/pdfs/GAFCHROMICEBT2TechnicalBrief-Rev1.pdf

Welsh, A. D., Dixon-Brown, A., and Stedeford, J. B. H. (1983); *Calculation of dose distribution for iridium 192 implants*, Acta Radiol. Oncol., 22, 331-336, 1983

Williamson, J., Coursey, B., DeWerd, L., Hanson, W., Nath, R. and Ibbot, G. (1999); "Guidance to users of Nycomed Amersham and North American Scientific Inc, I-125 Interstitial Sources: *Dosimetry and calibrations changes: recommendations of the American Association of Physicist in Medicine Radiation Therapy Committee Ad Hoc Subcommittee on Low-Energy Seed Dosimetry*". Med. Phys. 26, 570-573.

Yu Y., Anderson L. L., Li Z., Mellenberg D. E., Nath R., Schell M.C., Waterman F. M., Wu A., Blasleo J. C. (1999); *Permanent prostate seed implant brachytherapy: Report of the AAPM TG No. 64^(a)*, Med. Phys. 26;10,2054-2076.

APPENDIX**APPENDIX A: PERFORMANCE EVALUATION MEASUREMENTS**

A.1 LATERAL DISTANCE MEASUREMENTS B / mm				
positions/mm	B1-B2	B2-B3	B3-B4	B4-B5
0.50	10.15	9.94	9.99	10.02
1.00	10.17	10.09	10.07	10.17
1.50	10.09	10.17	9.95	10.17
2.00	10.17	9.95	10.16	10.23
2.50	10.09	10.09	10.09	10.23
3.00	9.94	9.94	10.10	10.02
3.50	10.02	10.30	10.10	10.30
4.00	10.23	10.23	10.30	10.09
4.50	10.10	10.15	10.17	10.10
5.00	10.17	10.09	10.23	9.95
5.50	10.23	10.43	10.35	10.30
6.00	10.17	10.30	10.09	10.30
6.50	10.02	10.09	10.10	10.03
7.00	10.09	10.09	10.09	10.03
7.50	10.03	10.03	9.95	10.10
8.00	10.10	10.23	10.03	10.09
8.50	10.15	10.09	10.03	10.03
9.00	10.09	10.13	10.09	10.09
9.50	10.29	10.09	10.03	10.09
10.00	10.15	10.03	10.22	10.09
10.50	10.01	10.09	10.10	10.03
MEAN	10.11714	10.12143	10.10667	10.11714
STD	0.084448	0.123624	0.103554	0.103157

A.2 LATERAL DISTANCE MEASUREMENT, F / mm

POSITIONS	F1-F2	F2-F3	F3-F4	F4-F5
0.50	9.95	10.09	10.17	10.08
1.00	10.09	10.09	10.15	10.57
1.50	10.10	10.23	10.02	10.17
2.00	10.17	10.23	10.10	10.23
2.50	9.94	10.10	10.23	10.30
3.00	10.02	10.30	10.15	9.95
3.50	10.33	10.12	10.09	10.23
4.00	10.10	10.01	10.23	9.95
4.50	10.17	10.23	10.23	10.30
5.00	9.95	10.10	10.03	9.95
5.50	10.17	10.17	10.08	9.64
6.00	10.29	10.09	10.02	10.29
6.50	10.10	10.02	10.09	9.95
7.00	10.03	10.02	10.02	10.03
7.50	10.02	10.03	10.10	9.95
8.00	10.09	10.09	10.09	10.09
8.50	10.09	10.22	10.09	10.09
9.00	9.95	9.95	10.09	10.03
9.50	10.16	10.08	10.02	10.10
10.00	10.15	10.03	10.16	10.09
10.50	10.09	10.09	10.09	10.09
MEAN	10.09333	10.10905	10.10714	10.09905
STD DEV	0.104897	0.090217	0.068785	0.188465

A.3 TEMPLATE GRID ALIGNMENT / mm

POSITIONS	4DR	4DT	6AR	6AT	6GR	6GT
1	2.05	1.45	2.67	1.05	1.85	1.64
2	2.01	1.44	2.66	1.03	1.84	1.63
3	2.00	1.45	2.65	1.06	1.82	1.62
4	2.04	1.46	2.68	1.06	1.87	1.65
5	2.02	1.44	2.68	1.05	1.86	1.66
MEAN	2.024	1.448	2.668	1.05	1.848	1.64
STD	0.020736	0.008367	0.013038	0.012247	0.019235	0.015811

A.4 AXIAL MEASUREMENTS /				
mm				
POSITION/cm	B-C	B-D	B-E	B-F
0.50	10.10	20.03	29.60	39.73
1.00	10.02	20.03	29.80	39.93
1.50	10.08	20.10	29.33	39.80
2.00	10.10	19.90	29.00	39.00
2.50	10.02	19.90	30.00	39.33
3.00	10.10	20.03	29.33	39.33
3.50	10.00	20.10	29.33	40.00
4.00	10.08	19.90	30.00	40.00
4.50	10.10	20.03	29.33	39.80
5.00	10.30	20.03	29.67	39.27
5.50	10.08	20.10	29.40	39.07
6.00	10.10	20.03	30.00	39.33
6.50	10.02	20.10	29.67	40.00
7.00	10.02	19.90	29.33	39.00
7.50	10.02	19.97	30.00	39.00
8.00	10.08	19.97	29.33	39.67
8.50	10.08	20.03	29.33	40.00
9.00	10.10	20.10	30.00	39.33
9.50	10.02	20.10	29.80	40.00
10.00	10.02	19.97	29.00	39.33
10.50	10.02	19.97	29.53	39.33
MEAN	10.06952	20.01381	29.56095	39.53571
STD DEV	0.06469	0.072765	0.326572	0.376239

APPENDIX B: TPS DOSE VERIFICATION TESTS

B 1. CALIBRATION POINT
MEASUREMENTS

Positions/cm	Current/mA
0.00	193.53
0.50	196.95
1.00	198.93
1.50	199.82
2.00	200.73
2.50	201.65
3.00	201.99
3.50	201.11
4.00	200.39
4.50	198.37
5.00	196.34
5.50	191.62
6.00	186.17
6.50	181.00
7.00	169.56
7.50	150.14
8.00	121.56

B.2 Dose at calculating point.

air kerma (U)	Activity (mCi)	Calc.pt 1	calc. pt 2	calc.pt 3	calc.pt.4	calc pt 5	calc.pt.6
0.329	0.249	99.43916	78.42501	74.17208	62.37006	116.08670	77.78705
0.325	0.246	102.7052	77.88729	71.57789	70.05199	102.25480	65.42144
0.321	0.243	110.2407	81.32150	78.89389	78.02535	137.73500	101.70250
0.318	0.240	127.8085	86.02254	77.95298	63.55792	131.57330	80.03935
0.314	0.238	98.41871	76.05762	58.79433	40.88791	90.04703	90.96304
0.310	0.235	94.40687	70.02161	64.26149	51.87403	102.18680	67.47127
0.307	0.232	82.78204	68.05762	63.75289	54.41916	90.74928	57.71087
0.303	0.229	92.59264	69.64221	68.24239	57.35078	102.00090	57.71087
0.300	0.226	86.94777	68.41225	63.34385	54.04600	94.76747	61.23974
0.296	0.224	78.61672	61.63793	56.01971	46.69174	86.82820	54.43124

B.3.		GAFCHROMIC FILM MEASUREMENTS				
A-	CALC.					
0.249	Pt	AREA	MEAN	StdDEV	SKEW	
	X6	1344	70.479	6.550	-1.068	
	X5	1344	61.460	3.519	-3.087	
	X1	1344	64.947	3.977	-1.901	
	X2	1344	70.295	2.498	-1.942	
	X3	1344	71.551	2.355	-5.531	
	X4	1344	75.455	3.833	-0.506	
	CALC.					
B- 0.246	Pt	AREA	MEAN	StdDEV	SKEW	
	X6	1344	74.379	5.914	-0.236	
	X5	1344	64.318	2.682	-2.630	
	X1	1344	64.219	2.627	-1.680	
	X2	1344	71.036	2.190	0.114	
	X3	1344	72.353	2.100	-3.769	
	X4	1344	75.568	3.922	-0.747	
	CALC.					
C- 0.243	Pt	AREA	MEAN	StdDEV	SKEW	
	X6	1344	64.440	4.939	0.419	
	X5	1344	57.608	2.216	-2.005	
	X1	1344	62.624	4.734	0.808	
	X2	1344	69.478	2.535	-1.941	
	X3	1344	70.175	2.456	-3.381	
	X4	1344	75.946	4.375	0.140	
	CALC.					
D-	CALC.					
0.240	Pt	AREA	MEAN	StdDEV	SKEW	
	X6	1344	69.836	6.235	-0.504	
	X5	1344	58.639	2.951	-2.403	
	X1	1344	59.293	3.450	-1.473	
	X2	1344	68.212	2.548	-1.581	
	X3	1344	70.431	2.344	-4.039	
	X4	1344	75.030	4.364	-0.018	
	CALC.					
E- 0.238	Pt	AREA	MEAN	StdDEV	SKEW	
	X6	1344	66.954	3.180	-2.975	

X5	1344	67.182	2.424	-1.497
X1	1344	73.043	3.206	-7.150
X2	1344	74.039	1.941	-5.895
X3	1344	76.785	3.655	-0.625
X4	1344	88.542	4.243	-0.702

		CALC.			
F- 0.235	Pt	AREA	MEAN	StdDEV	SKEW
	X6	1344	73.684	6.723	-0.550
	X5	1344	64.333	2.483	-4.215
	X1	1344	66.117	3.077	-0.902
	X2	1344	73.501	2.582	-1.772
	X3	1344	74.782	2.496	-1.410
	X4	1344	79.606	3.954	-0.098

		CALC.			
H- 0.232	Pt	AREA	MEAN	StdDEV	SKEW
	X6	1344	77.204	6.863	-0.635
	X5	1344	67.007	2.542	-1.285
	X1	1344	69.077	2.964	-1.286
	X2	1344	74.161	2.710	-1.285
	X3	1344	74.961	2.011	-2.179
	X4	1344	78.527	3.880	-1.178

		CALC.			
I- 0.229	Pt	AREA	MEAN	StdDEV	SKEW
	X6	1344	73.655	6.170	-0.203
	X5	1344	64.374	2.253	-1.519
	X1	1344	66.554	2.669	-0.526
	X2	1344	73.627	2.526	-0.726
	X3	1344	73.428	2.477	-0.894
	X4	1344	77.345	3.982	-0.498

		CALC.			
J- 0.226	Pt	AREA	MEAN	StdDEV	SKEW
	X6	1344	75.867	9.824	-2.279
	X5	1344	66.031	1.858	-0.627
	X1	1344	67.971	2.814	-2.13
	X2	1344	73.372	2.115	-1.274
	X3	1344	75.106	2.096	-2.546
	X4	1344	78.682	4.216	-0.374

		CALC.			
G- 0.224	Pt	AREA	MEAN	StdDEV	SKEW

X6	1344	78.522	7.371	-0.920
X5	1344	68.002	2.650	-1.462
X1	1344	70.24	3.038	-1.574
X2	1344	75.721	2.440	-1.899
X3	1344	77.874	1.907	-1.786
X4	1344	81.977	4.710	-1.368

B.4 Calibrated film
dosimetry

Mean	Gaf.dose(cGy)	%error
117.77	9.532243	0.000000
95.128	26.04383	-4.17534
82.231	46.168220	7.663551
70.760	76.822760	-2.43035
65.450	97.243400	2.756596
58.909	130.005800	-4.00460
54.300	159.521200	-6.34746
53.000	168.997700	3.429886
49.208	199.979700	0.010158
46.020	230.381000	-2.39154
45.800	232.641900	6.943245
42.231	272.579900	0.880036
39.648	305.696800	-1.89893
38.112	327.267600	-0.69774

APPENDIX C: SUGGESTED QC PROGRAM

Test	Minimum frequency	Action level
Depth of penetration	Annual	Change $> \pm 1$ cm from baseline (findings)
Axial resolution	Annual	Change $> \pm 1$ mm from baseline (findings)
Lateral resolution	Annual	Change $> \pm 1$ mm from baseline (findings)
Axial distance	Annual	Error $> \pm 2$ mm or 2%
Lateral distance	Annual	Error $> \pm 3$ mm or 3%
Volume measurement	Annual	Error $> \pm 5\%$
Physical/ internal grid alignment	Annual	Error $> \pm 3$ mm
Source strength calibration	Each use	$\pm 5\%$